Schizophrenia Bulletin
https://doi.org/10.1093/schbul/sbae221

Blunted Ventral Striatal Reactivity to Social Reward Is Associated with More Severe Motivation and Pleasure Deficits in Psychosis

Alexander J. Shackman[1,2,3]; Jason F. Smith[1]; Ryan D. Orth[1]; Christina L. G. Savage[1]; Paige R. Didier[1]; Julie M. McCarthy[4,5]; Melanie E. Bennett[6]; Jack J. Blanchard[*,1]

[1]Department of Psychology, University of Maryland, College Park, MD 20742, United States; [2]Neuroscience and Cognitive Science Program, University of Maryland, College Park, MD 20742, United States; [3]Maryland Neuroimaging Center, University of Maryland, College Park, MD 20742, United States; [4]Division of Psychotic Disorders, McLean Hospital, Belmont, MA 02478, United States; [5]Department of Psychiatry, Harvard Medical School, Boston, MA 02115, United States; [6]Department of Psychiatry, University of Maryland School of Medicine, Baltimore, MD 21201, United States

J. F. Smith and J. J. Blanchard contributed equally.

[*]To whom correspondence should be addressed: Jack J. Blanchard, Department of Psychology, 4094 Campus Drive, College Park, MD 20742, United States (jblancha@umd.edu)

***Background and Hypothesis*: Among individuals living with psychotic disorders, social impairment is common, debilitating, and challenging to treat. While the roots of this impairment are undoubtedly complex, converging lines of evidence suggest that social motivation and pleasure (MAP) deficits play a central role. Yet most neuroimaging studies have focused on monetary rewards, precluding decisive inferences.**

***Study Design*: Here we leveraged parallel social and monetary incentive delay functional magnetic resonance imaging paradigms to test whether blunted reactivity to social incentives in the ventral striatum—a key component of the distributed neural circuit mediating appetitive motivation and hedonic pleasure—is associated with more severe MAP symptoms in a transdiagnostic adult sample enriched for psychosis. To maximize ecological validity and translational relevance, we capitalized on naturalistic audiovisual clips of an established social partner expressing positive feedback.**

***Study Results*: Although both paradigms robustly engaged the ventral striatum, only reactivity to social incentives was associated with clinician-rated MAP deficits. This association remained significant when controlling for other symptoms, binary diagnostic status, or striatal reactivity to monetary incentives. Follow-up analyses suggested that this association predominantly reflects diminished activation during the presentation of social reward.**

***Conclusions*: These observations provide a neurobiologically grounded framework for conceptualizing the social-anhedonia symptoms and social impairments that characterize many individuals living with psychotic disorders and underscore the need to develop targeted intervention strategies.**

Key words: fMRI; incentive delay paradigm; negative symptoms; psychosis/psychotic spectrum; schizophrenia; social anhedonia/avolition.

Introduction

Among individuals living with schizophrenia and other psychosis spectrum disorders and those at-risk for developing these disorders, social impairments are common, debilitating, and challenging to treat, underscoring the need to clarify the underlying neurobiology.[1–8] While the roots of social impairment are undoubtedly complex and multiply determined, converging lines of laboratory and experience-sampling data suggest that motivation and pleasure (MAP) symptoms play a key role.[3,9–19]

MAP deficits are often conceptualized in terms of blunted reactivity to social rewards, including reduced motivation to seek out and engage in social interactions (*amotivation/avolition*) and diminished hedonic pleasure when interactions do occur (*anhedonia*).[3,13,20–24] To date, only a handful of psychosis studies have examined potential alterations in neural reactivity to social rewards.[25] Two small case-control studies provide preliminary evidence of aberrant reactivity to social incentives in the ventral striatum (**Figure 1**)—a key neural hub for appetitive motivation ("wanting") and hedonic pleasure

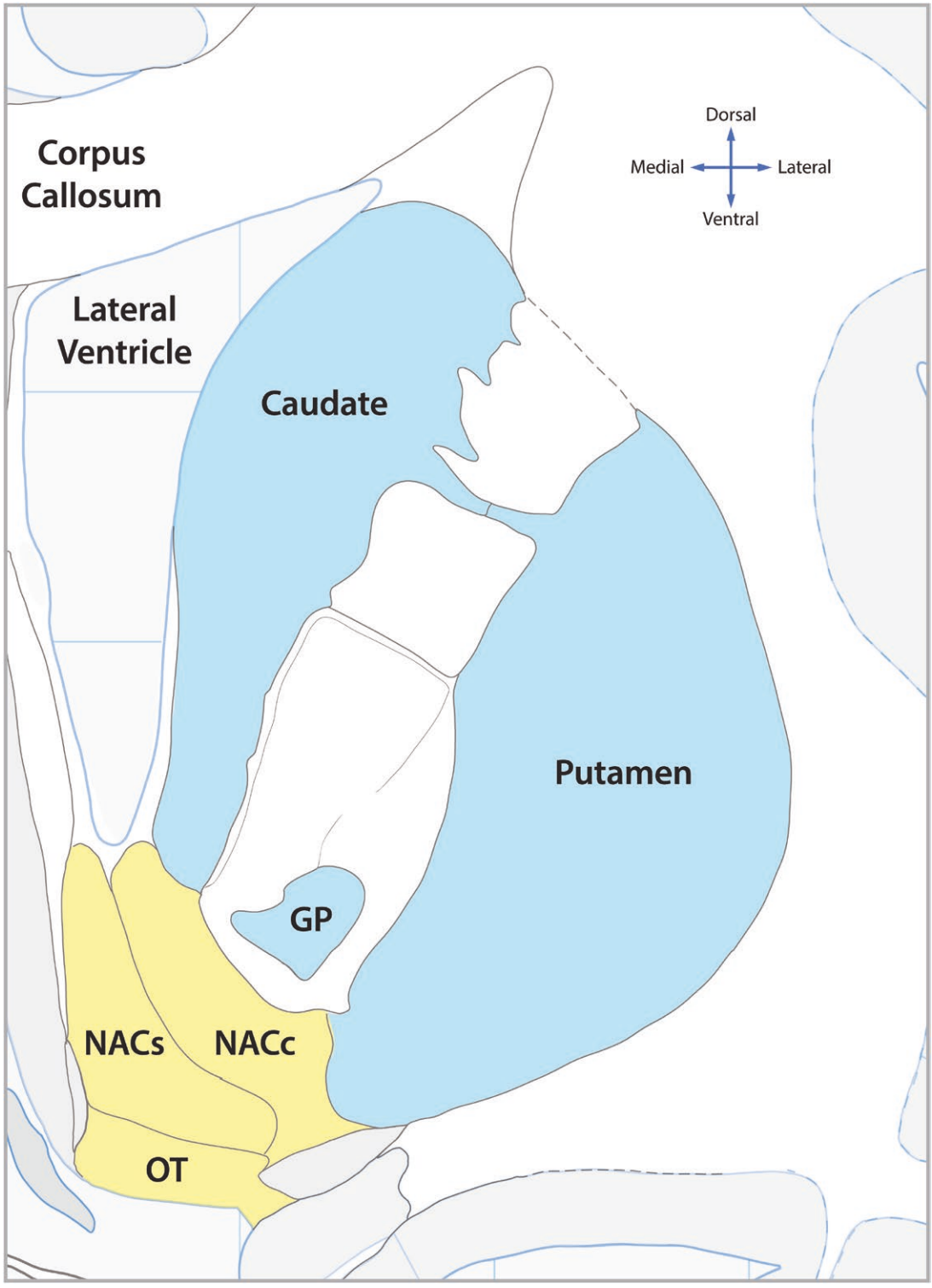

Figure 1. The Human Ventral Striatum. The Ventral Striatum Includes the Nucleus Accumbens and Olfactory Tubercle.[26] The Accumbens Can, in Turn, be Chemoarchitectonically Divided Into 2 Major Divisions, the Shell and Core, With the Shell Marked by Stronger Expression of Mu and Kappa Opioid Receptors and D1 and D3 Dopamine Receptors, and Weaker Expression of D2 Dopamine Receptors.[27,28] Mechanistic Work in Rodents Indicates That Both Divisions are Critically Involved in Dopamine-Mediated Appetitive Motivation ("wanting" Reward), Whereas Only the Medial Shell is Involved in Opioid/Cannabinoid-Mediated Hedonic Pleasure ("liking" Reward).[29,30] The Figure was Created with Reference to the Allen Institute and Mai atlases.[31,32] Abbreviations: GP, Globus Pallidus; NACc, Nucleus Accumbens Core; NACs, Nucleus Accumbens Shell; OT, Olfactory Tubercle.

("liking")[29,30,33]—among individuals with schizophrenia (n_{Cases} = 27).[34,35] Leveraging a much larger, transdiagnostic psychosis sample (n_{Cases} = 71), Jimenez et al. reported that diminished ventral striatum reactivity to social reward is associated with more severe MAP deficits and social-anhedonia symptoms.[36] Whether this association is reproducible remains unknown and whether it is specific to social reward remains unclear, as the authors only examined social incentives.

Here we used functional magnetic resonance imaging (fMRI) and parallel social and monetary incentive delay (SID/MID) paradigms to test the overarching hypothesis that blunted ventral striatum reactivity to social incentives will be associated with more severe MAP symptoms, indexed using gold-standard clinician ratings (**Figure 2**). The inclusion of the MID paradigm enabled us to clarify the specificity of this hypothesized association for the first time. Follow-up analyses were used to explore the relevance of other symptom dimensions, narrower reward facets (anticipation vs. presentation), and less intensively scrutinized brain regions. To ensure a broad spectrum of social impairment and MAP symptomatology, we adopted a Research Domain Criteria (RDoC) sampling strategy, focusing on a transdiagnostic community sample that was heavily enriched for psychosis (**Table 1**).[37,38] Most participants were on a stable regimen of outpatient treatment, enhancing clinical relevance. To date, clinical neuroimaging studies of social reward have relied almost exclusively on static photographs of positive facial expressions posed by unfamiliar adult models (ie, strangers). To maximize ecological validity and translational relevance,[25,39] we instead capitalized on pre-recorded audiovisual clips of an established social partner expressing varying degrees of social reward. As shown in **Figure 2**, we used the Social Affiliation Enhancement Task (SAET) to cultivate a sense of affiliation with an experimental partner just before the neuroimaging assessment.[11] Prior work by our group in a superset of the present sample confirms the validity of this approach, demonstrating that the SAET significantly enhances affiliative feelings, perceived closeness, and willingness to interact with the partner.[15] This novel naturalistic approach enabled us to manipulate the intensity of nonverbal (facial expressions and gestures), paralinguistic (vocal intonation), and verbal (praise) indicators of social reward expressed by a social partner.

Methods

Study Overview

The present study stems from a larger project focused on the nature and neurobiology of social affiliative deficits in psychosis (R01-MH110462).[15,40–42] Participants completed 2 assessments: A baseline clinical session and a 2-phase laboratory session. At the baseline clinical session, eligibility was confirmed; participants provided informed written consent; and demographic, diagnostic, symptom, and other self-report data were acquired. Participants were instructed to abstain from taking sedatives/benzodiazepines for at least 12 hours prior to the MRI assessment. None of these individuals disclosed concerns or exhibited noteworthy withdrawal or rebound effects. The latency between the 2 sessions was <2 weeks (M = 6.5 days, SD = 2.9). During the 2-phase laboratory session, participants completed (1) the SAET outside the scanner, and (2) the SID/MID paradigms inside the scanner (**Figure 2**). Following the last scan, participants were debriefed and compensated. Procedures were approved by the University of Maryland, Baltimore Institutional Review Board.

Participants

Recruitment. To capture a broad spectrum of MAP deficits, maximizing range and statistical power, a mixed transdiagnostic adult sample—including both clinical and community participants—was recruited.[38] A modest number of psychiatrically healthy community participants was included (26.1%; **Table 1**) to ensure that the full range of affiliative function was captured.[38] Clinical participants were recruited from outpatient community mental health clinics in the Washington, DC-Baltimore metropolitan region. Community participants were recruited via online advertisements (eg, Craigslist).

Enrollment Criteria. General inclusion criteria included 18-60 years of age, English fluency, and normal or corrected-to-normal vision, and consent to be videotaped during study participation. General exclusion criteria included moderate or severe substance use disorder in the past 6 months or mild substance use disorder in the past month, indexed by the *Structured Clinical Interview for DSM-5 Research Version* (SCID-5-RV)[43]; standard MRI contraindications (see below for details); lifetime neurological, developmental, or cognitive disorder, indexed by medical history or cognitive testing; or a lifetime history of serious head injury. Clinical inclusion criteria included a lifetime psychotic disorder (**Table 1**), clinical stability (ie, no inpatient hospitalizations in the past 3 months and no changes in psychoactive medication in the past month), and indexed by medical history. Community inclusion criteria included absence of current psychiatric diagnoses or medication (past 6 months), and absence of lifetime psychotic, mood, or personality disorder, indexed by SCID-5, and self-report.

Final Sample. A total of 120 participants completed the baseline clinical assessment. Of these, 12 did not attend the neuroimaging session due to psychiatric hospitalization (n = 1), study withdrawal (n = 10), or inclement weather (n = 1). The remaining 108 participants included a mixture of clinical (n = 87) and community (n = 21) participants. Of these, 39 participants were excluded from

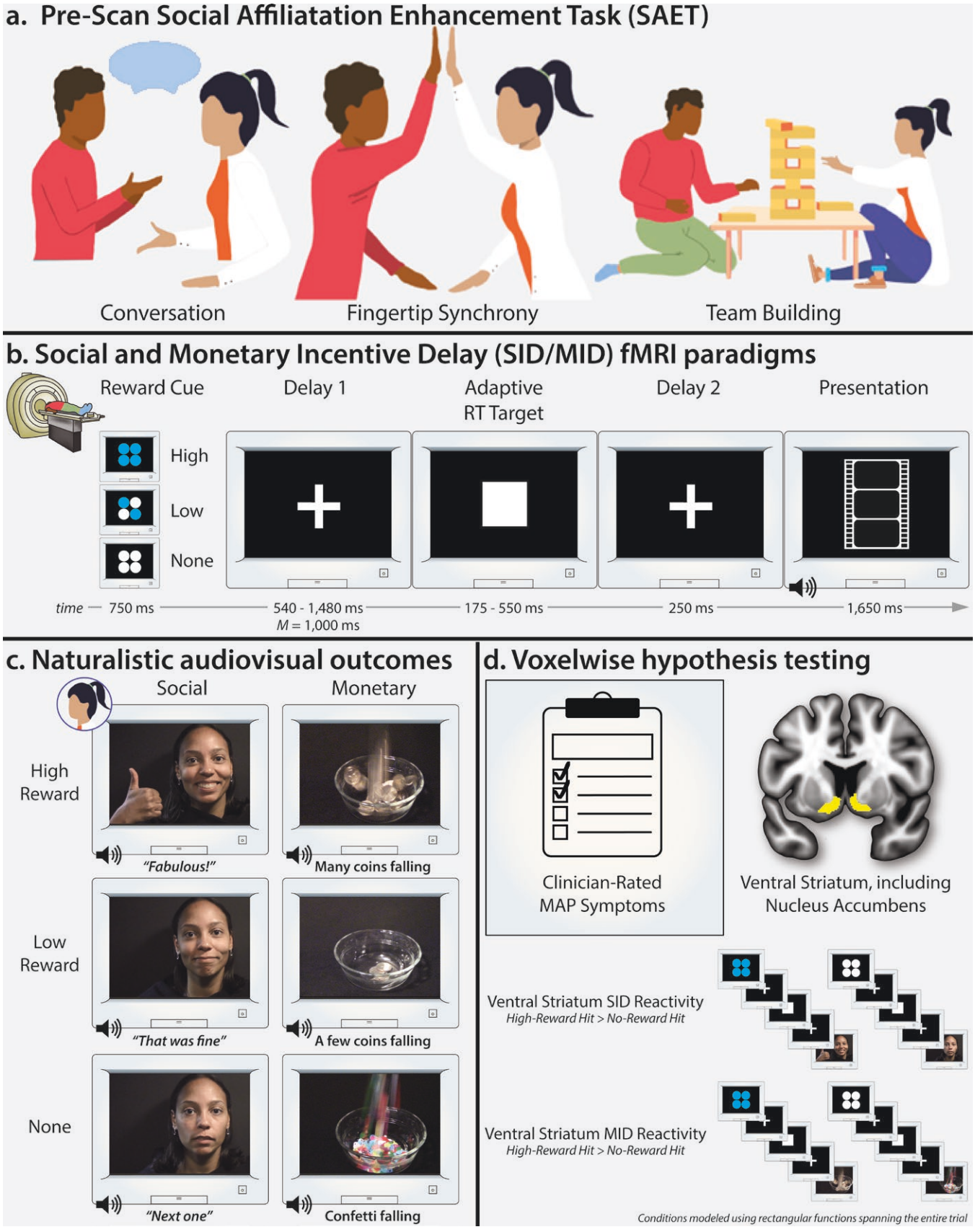

Figure 2. Conceptual Overview of the Study. (a) Pre-Scan Social Affiliation Enhancement Task (SAET). In the First Phase of the Session, Participants Completed the SAET, Which Encompasses 3 Tasks—Conversation, Implicit Fingertip Synchrony, and Team Building—Aimed at Promoting a Sense of Affiliation with an Experimental Partner. Prior Work Confirms the Validity of this Approach

in Psychotic Samples.[15] (b) Social and Monetary Incentive Delay (SID/MID) fMRI Paradigms. (c) Naturalistic Audiovisual Outcomes. To Maximize Ecological Validity and Translational Relevance, Short Audiovisual Clips Depicting Varying Degrees of Social or Monetary Reward Served as the Outcomes. For the SID Paradigm, the Clips Depicted the Individual Who Served as the Experimental Partner During the SAET. Staff Carefully Assessed Task Comprehension Prior to Scanning. Participants Were Fully Aware That the Clips Were Pre-Recorded. (d) Voxelwise Hypothesis Testing. Hypothesis Testing Focused on the Association between Clinician-Rated MAP Symptoms and Ventral Striatum Reactivity to Social and Monetary Reward, Indexed by the Cardinal High-Reward vs. No-Reward Contrast. Analyses Focused on Trials Where the Participant Responded Sufficiently Fast to Earn Reward ("hit"). For Primary Hypothesis Testing, Each Condition Was Modeled Using a Rectangular Function Spanning the Entire Trial. Abbreviations: fMRI, Functional Magnetic Resonance Imaging; MAP, Motivation and Pleasure; MID, Monetary Incentive Delay Paradigm; ms, Milliseconds; RT, Response Time; SID, Social Incentive Delay Paradigm.

Table 1. Sample Characteristics

Characteristic	Mean (*SD*) or *n* (%)
Age (years)	43.4 (12.0)
Sex	
Male	45 (65.2%)
Female	24 (34.8%)
Race	
African American	46 (66.7%)
White	16 (23.2%)
Asian	3 (4.3%)
More than one race	3(4.3%)
Not reported	1 (1.4%)
Ethnicity	
Non-Hispanic or Latino	65 (94.2%)
Hispanic or Latino	3 (4.3%)
Not reported	1 (1.4%)
Education (years)	13.0 (2.4)
Current employment	
Yes	25 (36.2%)
No	44 (63.8%)
Diagnosis	
Schizophrenia	22 (31.9%)
Schizoaffective, bipolar type	6 (8.7%)
Schizoaffective, depressive type	9 (13.0%)
Bipolar I with psychotic features	8 (11.6%)
MDD with psychotic features	6 (8.7%)
No diagnosis	18 (26.1%)
Age of first psychiatric treatment (clinical)	20.0 (9.2)
Medications (% clinical participants)	
Atypical antipsychotic	34 (66.7%)
Typical antipsychotic	6 (11.8%)
Atypical and typical antipsychotic	3 (5.9%)
Antipsychotic (chlorpromazine) dose equivalent	266.5 (348.5)
Antidepressant	23 (45.1%)
Mood stabilizer	22 (43.1%)

N = 69. Abbreviations: MDD, major depressive disorder.

analyses due to study withdrawal ($n = 8$), MRI safety concerns ($n = 5$), poor fit in the scanner ($n = 3$), technical problems ($n = 8$), excessive movement ($n = 1$; see below), or inadequate task compliance (hit-rate <10% during any scan; $n = 14$), and yielding a final sample of 69 individuals (**Table 1**). The final sample ($n = 69$) did not significantly differ from the excluded participants ($n = 39$) in terms of sex, race, ethnicity, age, employment status, or education ($P > .05$). The 2 groups also did not differ on symptom severity, as indexed by the *Clinical Assessment Interview for Negative Symptoms* (CAINS) and *Brief Psychiatric Rating Scale* (BPRS) ($P > .05$; see below). In the final sample, clinical and community participants also did not differ in any of the demographic characteristics ($P > .05$) except for a small but significant difference in years of education ($M_{Clinical}$: 12.5 years; $M_{Community}$: 14.6 years; $t(67) = 3.34$, $P = .002$).

Clinical Assessments

Diagnoses. To confirm eligibility and diagnosis, all participants completed the SCID-5-RV. Detailed assessments were determined by the SCID-5 screener and could include the psychotic disorders, mood, and substance-use modules. Assessments were conducted by well-trained Master's level interviewers supervised by doctoral-level clinical psychologists. Co-morbidities were not systematically assessed.

Clinician-Rated Symptoms. The CAINS is a well-established 13-item interview that indexes deficits in MAP (9 items; eg, amotivation, asociality, and anhedonia; α = .80) and *Expression* (4 items; eg, affective flattening and alogia; α = .87) (**Table 2**).[10,44] Four of the nine MAPS items are squarely centered on MAP deficits in the social sphere (eg, desire for close interpersonal relationships), whereas the remaining 5 are focused on occupational, academic, and recreational activities, which often include a blend of social and non-social reward. The 9 items were robustly inter-correlated (α = .80) and an ad hoc score based on the 4 overtly social items was strongly correlated with the total score ($r = 0.87$), suggesting that the total score is strongly infused with MAP deficits of a social nature. The CAINS has been extensively validated and successfully deployed in a variety of clinical and non-clinical populations.[10,15,34,36,45,46] Elevated MAP deficits are associated with reduced desire for close relations and social engagement,[10] impaired social functioning,[10,12,47] and diminished affiliative responses to semi-structured social encounters.[11,15] For hypothesis testing, the MAP scale served as the primary index of social amotivation and anhedonia. The expanded BPRS is a 24-item interview that was used to index *Positive Symptoms* (8 items; α = .69), *Depression/Anxiety* (4 items; α = .74), and *Agitation* (6 items; α = .53).[48,49]

Self-Reported Social Function. The 7-item *Interpersonal Relationships* scale from the *Specific Levels of Functioning*

Table 2. Descriptive Statistics for Symptoms and Social Function

Scale (instrument)	*M* (*SD*)	Range
Motivation and pleasure (CAINS)	11.5 (6.7)	1-34
Expression (CAINS)	5.5 (3.6)	0-14
Positive symptoms (BPRS)	12.5 (6.0)	8-31
Depression/anxiety (BPRS)	7.7 (4.1)	4-19
Agitation (BPRS)	7.5 (2.3)	6-19
Interpersonal relationships (SLOF)	27.1 (6.3)	11-35

N = 69. Abbreviations: BPRS, Brief Psychiatric Rating Scale; CAINS, Clinical Assessment Interview for Negative Symptoms; SLOF, Specific Levels of Functioning.

(SLOF) instrument was used to index interpersonal functioning (α = .89) (**Table 2**).[50,51] Consistent with prior studies, in the current sample more severe MAP symptoms were associated with poorer interpersonal functioning ($r(67) = -0.56$, $P < .001$).

Social Affiliation Enhancement Task

The SAET encompasses a validated suite of procedures for cultivating social rapport, trust, and affiliation (**Figure 2a**) (for details, see Refs. [11,15]). Prior work by our group demonstrates that the SAET significantly enhances affiliative feelings, perceived closeness, and willingness to interact with the partner,[15] consistent with work using similar paradigms.[18] As in previous work by our group, the affiliative partner was always the opposite sex of the participant.[11,15]

SID/MID fMRI Paradigms

Overview and Procedures. As shown in **Figure 2b**, parallel incentive-delay paradigms were used to probe neural reactivity to social and monetary reward.[52,53] Both paradigms took the form of balanced 3-condition (*Reward Level:* High, Low, and None) randomized, event-related, and repeated-measures designs (paradigm order counterbalanced; 2 scans/paradigm; and 22 trials/condition/scan). The general task structure, timing, and procedures were identical across paradigms and similar to prior work in clinical and healthy populations (**Figure 2b**). Trial timing and randomization were optimized via simulations to maximize the detection of global differences in reward reactivity, while remaining mindful of participant burden and tolerability (variance inflation factors <2.55). Participants were completely informed about the task structure and contingencies prior to scanning. They were instructed that the goal of both paradigms was to maximize reward and that this was contingent on the speed of their response to a briefly presented visual target. Responses were made using the first digit of the dominant hand and an MRI-compatible response-pad (MRA, Washington, PA). To maintain a comparable level of difficulty across paradigms, trials, and participants, the response-time threshold (signaled by the duration of the target presentation) was adaptively adjusted on a trial-by-trial basis (±25 ms, minimum = 175 ms, maximum = 600 ms; target hit-rate: M = 66%, Range = 60%-73%). Too-slow responses ("misses") triggered the presentation of the no-reward audiovisual clips (**Figure 2c**). No-reward clips were presented on all no-reward trials, irrespective of response time (hit/miss). Prior to scanning, participants practiced abbreviated versions of the paradigms and staff provided feedback as necessary to ensure participant comprehension. Behavioral data from the practice tasks was used to initialize the response-time thresholds for the neuroimaging experiment. Stimulus presentation and behavioral data acquisition were controlled using *Presentation* (version 19.0, Neurobehavioral Systems, Berkeley, CA). Hit-rate was matched across paradigms, $t(68) = 0.85$, $P = .40$ (*SID:* M = 64.8%, SD = 0.08; *MID:* M = 65.5%, SD = 0.05) and unrelated to the severity of MAP symptoms, $|r| < 0.08$, $P > .51$.

SID Outcomes. Prior neuroimaging studies of social reward in psychosis have relied on static photographs of positive facial expressions posed by unfamiliar adult models.[34–36] Here we capitalized on naturalistic audiovisual clips of the experimental partner from the SAET, enhancing ecological validity, and translational relevance (**Figure 2**). Building on preclinical work in university students,[54] this approach enabled us to manipulate the intensity of nonverbal (facial expressions and gestures), paralinguistic (vocal intonation), and verbal (praise) indicators of social reward expressed by a psychologically meaningful social partner. High-reward clips featured large open-mouth smiles, thumbs-up gestures, and verbal feedback indicative of exceptional performance (*Amazing!, Awesome!, Fabulous!, Fantastic!,* and *Spectacular!*) and expressed in an ebullient manner (**Figure 2c**). Low-reward clips featured small closed-mouth smiles and verbal feedback indicative of good performance (*Decent, That was cool, That was fine, That was nice, and That was neat*), expressed in a mildly positive manner. No-reward clips were devoid of facial expressions and gestures; instead, the partner simply instructed the participant to prepare for the next trial (*Continue, Get ready, Keep going, Next one, and Proceed*) in a neutral monotone. There was no deception or attempt to convince participants that the social feedback was occurring in real time. Participants were fully aware that the videoclips of the SAET partner were pre-recorded.

MID Outcomes. As shown in **Figure 1c**, high-reward audiovisual clips featured 10 coins falling into a bowl, low-reward clips featured 4 coins falling in a bowl, and no-reward trials featured confetti falling into a clear bowl. In addition to the audiovisual clips, successful performance of the high- and low-reward MID trials was incentivized by $1.00 and $0.20, respectively, in monetary

compensation. On average, participants earned $32.59 (*SD* = 1.25).

MRI Data Acquisition

MRI data were acquired using a Siemens Magnetom TIM Trio 3 Tesla scanner (32-channel head-coil). Foam inserts were used to mitigate potential motion artifact. To further mitigate motion artifact, for the final 14 participants, a strip of medical tape was positioned just above the forehead, and providing tactile feedback.[55] Sagittal T1-weighted anatomical images were acquired using a magnetization-prepared rapid acquisition gradient echo sequence (TR = 2400 ms; TE = 2.01 ms; inversion = 1060 ms; flip = 8°; slice thickness = 0.8 mm; in-plane = 0.8 mm^2; matrix = 300 × 320; field-of-view = 240 × 256). A T2-weighted image was collected co-planar to the T1-weighted image (TR = 3200 ms; TE = 564 ms; flip = 120°). To enhance resolution, a multi-band sequence was used to collect oblique-axial echo planar imaging (EPI) volumes (acceleration = 6; TR = 1250 ms; TE = 39.4 ms; flip = 36.4°; slice thickness = 2.2 mm, number slices = 66; in-plane = 2.1875 mm^2; matrix = 96 × 96; 355 volumes × 4 scans). Images were collected in the oblique axial plane (approximately −20° relative to the AC-PC plane) to minimize potential susceptibility artifacts. The scanner automatically discarded 7 volumes prior to the first recorded volume. To enable fieldmap correction, 2 oblique-axial spin echo (SE) images were collected in each of 2 opposing phase-encoding directions (rostral-to-caudal/caudal-to-rostral) co-planar to the functional volumes (TR = 7220 ms; TE = 73 ms). Respiration and pulse were acquired using a respiration belt and photo-plethysmograph affixed to the first digit of the non-dominant hand. Participants were continuously monitored using an MRI-compatible eye-tracker (Eyelink 1000; SR Research, Ottawa, Ontario, Canada) and the AFNI real-time motion plugin.[56] Eye-tracking data were not recorded.

MRI Data Processing Pipeline

Methods were optimized to minimize spatial normalization error and other potential sources of noise, and are similar to those detailed in other recent reports by our group.[15,57,58] Data were visually inspected before and after processing for quality assurance. All participants provided 4 usable scans.

Anatomical Data. T1-weighted images were inhomogeneity corrected using *N4*[59] and filtered using *ANTS DenoiseImage*.[60] Brains were extracted using *BEaST*[61] and brain-extracted-and-normalized reference-brains.[62] Brain-extracted T1 images were normalized to a version of the brain-extracted 1-mm T1-weighted MNI152 (version 6) template modified to remove extracerebral tissue.[63] Normalization was performed using the diffeomorphic approach implemented in *SyN* (version 2.3.4).[60] T2-weighted images were rigidly co-registered with the corresponding T1 prior to normalization. The brain-extraction mask from the T1 was then applied. Tissue priors were unwarped to native space using the inverse of the diffeomorphic transformation.[64] Brain-extracted T1 and T2 images were segmented—using native-space priors generated in *FAST* (version 6.0.4)[65]—for subsequent use in T1-EPI co-registration (see below).

Fieldmap Data. SE images and *topup* were used to create fieldmaps. Fieldmaps were converted to radians, median-filtered, and smoothed (2-mm). The average of the motion- and distortion-corrected SE images was inhomogeneity corrected using *N4* and masked to remove extracerebral voxels using *3dSkullStrip* (version 20.2.14).

Functional Data. EPI files were de-spiked using *3dDespike*, slice-time corrected to TR-center using *3dTshift*, and motion corrected to the first volume using *ANTS* (12-parameter affine). Transformations were saved in ITK-compatible format for subsequent use.[66] The first volume was extracted and inhomogeneity corrected for EPI-T1 co-registration. The reference EPI volume was simultaneously co-registered with the corresponding T1-weighted image in native space and corrected for geometric distortions using boundary-based registration.[65] This step incorporated the previously created fieldmap, undistorted SE, T1, white matter image, and masks. To minimize potential normalization error, reference EPI volumes were spatially normalized to the MNI template using *SyN*, intensity standardized, and averaged to create a study-specific EPI template.[67–69] Normalized EPI reference volumes were then normalized to that template. To minimize incidental spatial blurring, the operations necessary to transform each EPI volume from native space to the reference EPI, from the reference EPI to the T1, from the T1 to the MNI template, and from the MNI template to the study-specific EPI template were concatenated and applied to the processed EPI data in a single step. Normalized EPI data were resampled (2 mm^3) using fifth-order b-splines and spatially smoothed (6-mm) using *3DblurInMask*.

fMRI Data Exclusions and Modeling

General Approach. For each participant, first-level modeling was performed using general linear models (GLMs) implemented in *SPM12* (version 7771), using the default autoregressive model and temporal band-pass filter set to the hemodynamic response function (HRF) and 128 s.[70] Consistent with past work,[15,57,58] nuisance variates included volume-to-volume displacement and its derivative, motion (6 standard parameters, global volume-to-volume displacement, and temporal derivatives), cerebrospinal

fluid signal, instantaneous pulse and respiration signals, and ICA-derived nuisance signals (eg, global motion).[71] Volumes with excessive volume-to-volume displacement (>0.66 mm) were censored. The inter-trial interval served as the implicit baseline.

Data Exclusions. Volume-to-volume ("framewise") displacement, averaged separately for each scan, was used to assess residual motion artifact. Participants showing consistently elevated motion across scans (>3 *SD*) were excluded from analyses ($n = 1$).

Modeling. For hypothesis testing purposes, reward signals were modeled using variable-duration rectangular ("box-car") regressors that spanned the entire trial, separately for each combination of reward level (High, Low, and None) and outcome (Hit/Miss) (**Figure 2b**). Regressors were convolved with a canonical HRF and its temporal derivative. Because the data were collected in different scans (order counterbalanced), the social and monetary paradigms were modeled separately.

To explore the relevance of finer differences in neural reward signaling, we separately modeled the anticipation and presentation phases of the trial using delta functions time-locked to the onset of the cue and outcome, respectively, for each combination of reward level and outcome (**Figure 2b**). Although our incentive-delay paradigms were not originally optimized for this modeling approach, collinearity proved acceptable (variance inflation factors <3.36).[72] Regressors were convolved with a canonical HRF.

Analytic Strategy

Overview. Analyses were implemented in SPSS (version 27.0.1; IBM, Armonk, NY), *SPM12*,[70] and in-house MATLAB code (version 9.14.0.2239454; The MathWorks, Natick, MA). Diagnostic procedures and data visualizations were used to confirm that test assumptions were satisfied[73] and key conclusions remained unchanged using robust regression (not reported).[74] Some figures were created using created using *R* (version 4.0.2),[75] *Rstudio* (version 1.2.1335),[76] *ggplot2* (version 3.4.1),[77] and *MRIcron* (version 1.0.20190902).[78] Clusters and peaks were labeled using the Harvard–Oxford atlas,[79–81] supplemented by descriptions of the orbitofrontal cortex, the ventral striatum, and its major divisions: The nucleus accumbens core, the nucleus accumbens shell, and the olfactory tubercle (**Figure 1**).[27,31,32,82–84] It merits comment that the term "ventral striatum" is often used in a more causal and imprecise way to refer to any region within the ventromedial portion of the basal ganglia (eg, pallidum).

Confirmatory Testing. Whole-brain voxelwise ("second-level") repeated-measures ("random effects") GLMs were used to confirm that the SID and MID tasks robustly engaged the ventral striatum, as indexed by the cardinal high-versus-no-reward contrast for hit trials. Significance was assessed using $P < .05$, whole-brain familywise error (FWE) corrected for cluster extent, and a cluster-defining threshold of $P < .001$.[85]

Hypothesis Testing. The overarching goal of this study was to test the hypothesis that blunted ventral striatum reactivity to social incentives is associated with more severe clinician-rated MAP symptoms. To do so, we used a standard voxelwise regression, with mean-centered CAINS MAP as the predictor, mean-centered sex and age as nuisance variates, and the high-versus-no-reward contrast as the outcome (**Figure 2d**), consistent with prior work.[33,35] Significance was assessed using $P < .05$, FWE corrected for the volume of the anatomically defined ventral striatum (**Figure 2d**).[86] The same approach was used to probe potential associations with ventral striatum reactivity to monetary incentives.

Specificity Analyses. When a significant association was observed, a voxelwise multiple regression was used to test whether ventral striatum reactivity to that incentive (eg, social) continued to explain significant variance in MAP symptoms when statistically controlling for mean-centered reactivity to the other incentive (eg, monetary), sex, and age ($P < .05$, ventral striatum FWE corrected). For a similar voxelwise-covariate approach.[87] Follow-up analyses allowed us to test whether MAP symptoms explain significant variance in ventral striatum reward signaling, over-and-above mean-centered affective flattening/alogia, positive symptoms, depression/anxiety, agitation, and binary diagnostic status (case vs. control; $P < .05$, ventral striatum FWE corrected). All of these analyses relied on the cardinal high versus no-reward contrast (hit trials). Follow-up analyses were used to confirm that significant MAP associations were in fact primarily due to blunted reactivity to high-reward trials ($P < .05$, uncorrected).

Secondary Analyses. The same general approach was used to explore the relevance of disaggregating striatal responses to the anticipation-versus-presentation of reward (see above for modeling details). Here again, when a significant association was detected, voxelwise multiple regression was used to test whether ventral striatum reactivity to that phase of the trial (eg, anticipation) continued to explain significant variance in MAP symptoms when statistically controlling for mean-centered reactivity to the other phase (eg, presentation), sex, and age ($P < .05$, ventral striatum FWE corrected). For a similar approach.[88]

Exploratory Analyses. Voxelwise regressions were used to explore potential associations between ventral striatum reward signaling and self-reported interpersonal functioning (*SLOF*; $P < .05$, ventral striatum FWE corrected), and to assess associations between MAP

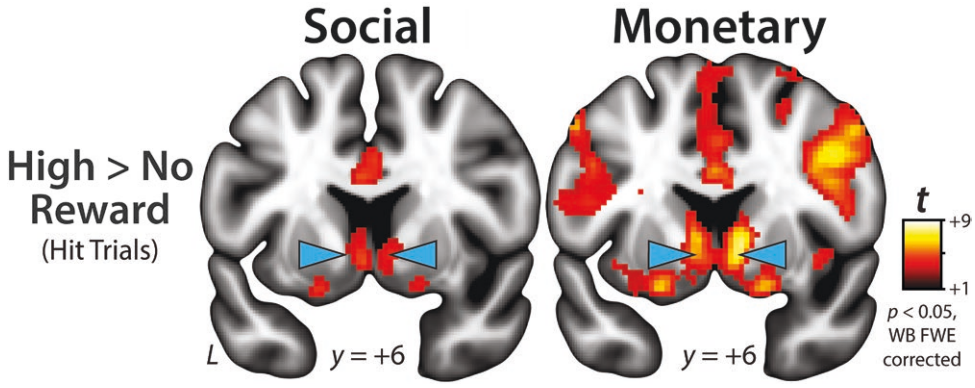

Figure 3. Social and Monetary Incentives Both Robustly Engage the Ventral Striatum. Figure Depicts Regions Showing Significantly Greater Activation During High-Reward Compared With No-Reward Hit Trials for the SID (Left) and MID (Right) paradigms ($P < .05$, Whole-Brain FWE Corrected). Each Condition was Modeled Using a Rectangular Regressor Spanning the Entire Trial. Arrows Indicate the Ventral Striatum. For detailed results, see Supplementary Tables S2–S5. Abbreviations: FWE, Familywise Error; L, Left Hemisphere; WB, Whole-Brain.

symptoms and reward signaling beyond the ventral striatum ($P < .05$, whole-brain FWE corrected).

Results

Social and Monetary Incentives Both Robustly Engage the Ventral Striatum

As a precursor to hypothesis testing, we used whole-brain voxelwise GLMs to determine whether the SID and MID paradigms had the expected neurophysiological consequences, as indexed by the cardinal high reward vs. no-reward contrast (hit trials). Consistent with work in healthy[89,90] and psychotic[23,91] samples, results confirmed that social and monetary incentives recruited an overlapping network of subcortical and cortical regions, including bilateral ventral striatum, thalamus, cingulate (subgenual, pregenual, and midcingulate), anterior insula, orbitofrontal cortex (posterior orbital gyrus), superior parietal lobule, and ventral visual cortex ($P < .05$, whole-brain FWE corrected; **Figure 3**; Supplementary Tables S1–S4). The less robust difference for the social task is consistent with prior work,[35] and it is what one would expect if the magnitude of activation is moderated by individual differences in MAP symptoms, as this unmodeled variance contributes to the error term of the between-condition test.

MAP Deficits are Associated with Blunted Ventral Striatum Reactivity to Social Incentives

We used a standard voxelwise regression to test whether ventral striatum reactivity to social incentives—indexed by the cardinal high-versus-no-reward contrast for hit trials—is associated with the severity of MAP symptoms (**Figure 2**). As shown in **Figure 4a**, results revealed a significant cluster in the left ventral striatum where this pattern was evident ($P < .05$, FWE corrected for the volume of the ventral striatum; controlling for mean-centered age and sex), with the peak lying in the region of the medial shell of the nucleus accumbens (NACs; cf. **Figure 1**). In contrast, a significant association was not evident for ventral striatum reactivity to monetary incentives. Consistent with this observation, a voxelwise multiple regression demonstrated that ventral striatum reactivity to social incentives continued to explain significant variance in MAP symptoms while statistically controlling for mean-centered reactivity to monetary incentives ($P < .05$, ventral striatum FWE corrected). The association between ventral striatum reactivity to social incentives and MAP symptoms also remained significant when individually controlling for other symptoms (affective flattening, positive symptoms, depression/anxiety, and agitation) or for binary diagnostic status (ie, case- vs. -control; $P < .05$, ventral striatum FWE corrected). Of course, these analyses relied on the difference in activation between high- and no-reward (hit) trials. Follow-up analyses confirmed that the association with MAP symptoms was predominantly due to reduced reactivity to high-reward social incentives (*high-reward:* $t(65) = -2.59$, $P = .01$, uncorrected; *no-reward:* $t(65) = 0.74$, $P = .46$, uncorrected). Taken together, these findings demonstrate that clinician-rated MAP deficits are selectively associated with blunted ventral striatum reactivity to naturalistic social incentives.

MAP Deficits are Associated with Ventral Striatum Reactivity to Social Reward Presentation

Using the same general analytic approach, secondary analyses enabled us to examine the potential relevance of disaggregating ventral striatum responses to the anticipation-versus-presentation of social reward (**Figure 1**). We began by using a whole-brain voxelwise GLMs to determine whether the 2 phases of the SID paradigm, here considered separately, recruit the ventral striatum. As shown in Supplementary Figure S1, significant

ventral striatum activation was only evident during the presentation of social rewards ($P < .05$, whole-brain FWE corrected). For completeness, detailed results for both paradigms can be found in Supplementary Tables S5–S12. Significant ventral striatum activation was not evident for the anticipation phase of the SID paradigm, even when using a more liberal small-volume threshold ($P < .05$, ventral striatum FWE corrected). Next, we used a voxelwise regression to determine whether ventral striatum activation during the presentation of social rewards is associated with more severe MAP symptoms. As shown in **Figure 4b**, this pattern was again evident in the medial NACs, overlapping the ventral striatum cluster identified in our primary analyses ($P < .05$, ventral striatum FWE corrected; **Figure 4a**). Ventral striatum activation during the *presentation* phase continued to explain significant variance in MAP symptoms when statistically controlling for mean-centered activation during the *anticipation* phase, sex, and age ($P < .05$, ventral striatum FWE corrected). In short, the severity of MAP deficits is selectively associated with diminished ventral striatum reactivity to the receipt of naturalistic social rewards.

Exploratory Analyses

Ventral striatum reactivity to social and monetary incentives was unrelated to variation in self-reported social functioning ($P > .05$, ventral striatum FWE corrected). Whole-brain voxelwise analyses did not detect any significant associations between MAP symptoms and reactivity to either social or monetary incentives outside of the ventral striatum ($P < .05$, whole-brain FWE corrected).

Discussion

The present results demonstrate that more severe clinician-rated MAP symptoms are associated with blunted ventral striatum reactivity to naturalistic social incentives (**Figure 4a**). This association remained significant when controlling for a variety of other symptoms (eg, diminished expressivity) or binary diagnostic status, underscoring the utility of conceptual models—such as RDoC and the Hierarchical Taxonomy of Psychopathology—centered on transdiagnostic symptom dimensions.[37,38,92,93] Although the ventral striatum was robustly engaged by both social and monetary incentives (**Figure 3**), as in prior work, striatal reactivity to monetary incentives was unrelated to MAP deficits. Likewise, in a simultaneous regression model, ventral striatum reactivity to social incentives was selectively and significantly associated with the severity of MAP symptoms, over-and-above variance explained by reactivity to monetary incentives. Secondary analyses demonstrated that diminished reactivity to the presentation of naturalistic social rewards was associated with greater MAP deficits in an overlapping region of the ventral striatum (**Figure 4b**), replicating and extending work focused on more conventional social-reward stimuli (photographs of unfamiliar smiling faces).[34,36] This association remained significant when controlling for activation during the earlier reward-anticipation phase, suggesting a preferential link between striatal reactivity to positive social feedback and MAP symptoms. Taken together, these observations provide a novel neurobiologically grounded framework for conceptualizing the social deficits that characterize many individuals living with psychotic disorders.

Clinical neuroscientists have long suspected that alterations in ventral striatum function might contribute to the pathophysiology of psychosis, but the specific mapping from the brain to symptomatology has only recently started to come into focus.[36,94,95] The present results indicate that more severe MAP symptoms are associated with blunted reactivity to the receipt of social reward in the region of the medial NACs, a division of the larger ventral striatum that is thought to play a mechanistically critical role in opioid/cannabinoid-mediated hedonic pleasure ("liking" reward)[29,30] (**Figure 1**). For example, preclinical neuroimaging research shows that acute administration of the opioid antagonist naloxone dampens both subjective pleasure and medial NACs reactivity to positive social stimuli (erotic photographs).[96] Paralleling our results, dampening was weak-to-nonexistent for monetary stimuli or for the anticipation of social stimuli. Taken together, these observations motivate the hypothesis that more severe MAP deficits reflect aberrant opioid/cannabinoid signaling in the medial NACs during normatively rewarding social interactions, manifesting as diminished feelings of pleasure. While the molecular neurobiology remains untested, prior work by our group supports the psychological component of this hypothesis, showing that individuals with more severe MAP symptoms experienced lower levels of positive affect and social affiliation and emitted fewer positive facial expressions during interactions with a social partner in the SAET, the same individual who served as the model for our naturalistic social-reward stimuli (**Figure 2**).[15] Outside of the laboratory, ecological momentary assessment research shows that more severe MAP symptoms are associated with less time spent with others and diminished positive affect in unstructured social contexts.[16] A key challenge for the future will be to clarify the origins and timing of social-reward deficits in psychosis. In particular, it will be fruitful to determine if blunted ventral striatum reactivity to social reward precedes and promotes the emergence of frank psychosis or whether it reflects a consequence of the social isolation and rejection often experienced by individuals with psychotic disorders.[2,97–99] It will also be useful to determine whether emerging cognitive-behavioral treatments targeting social affiliation and connectedness (eg, positivity amplification) rescue ventral striatum reactivity to social incentives.[18,100]

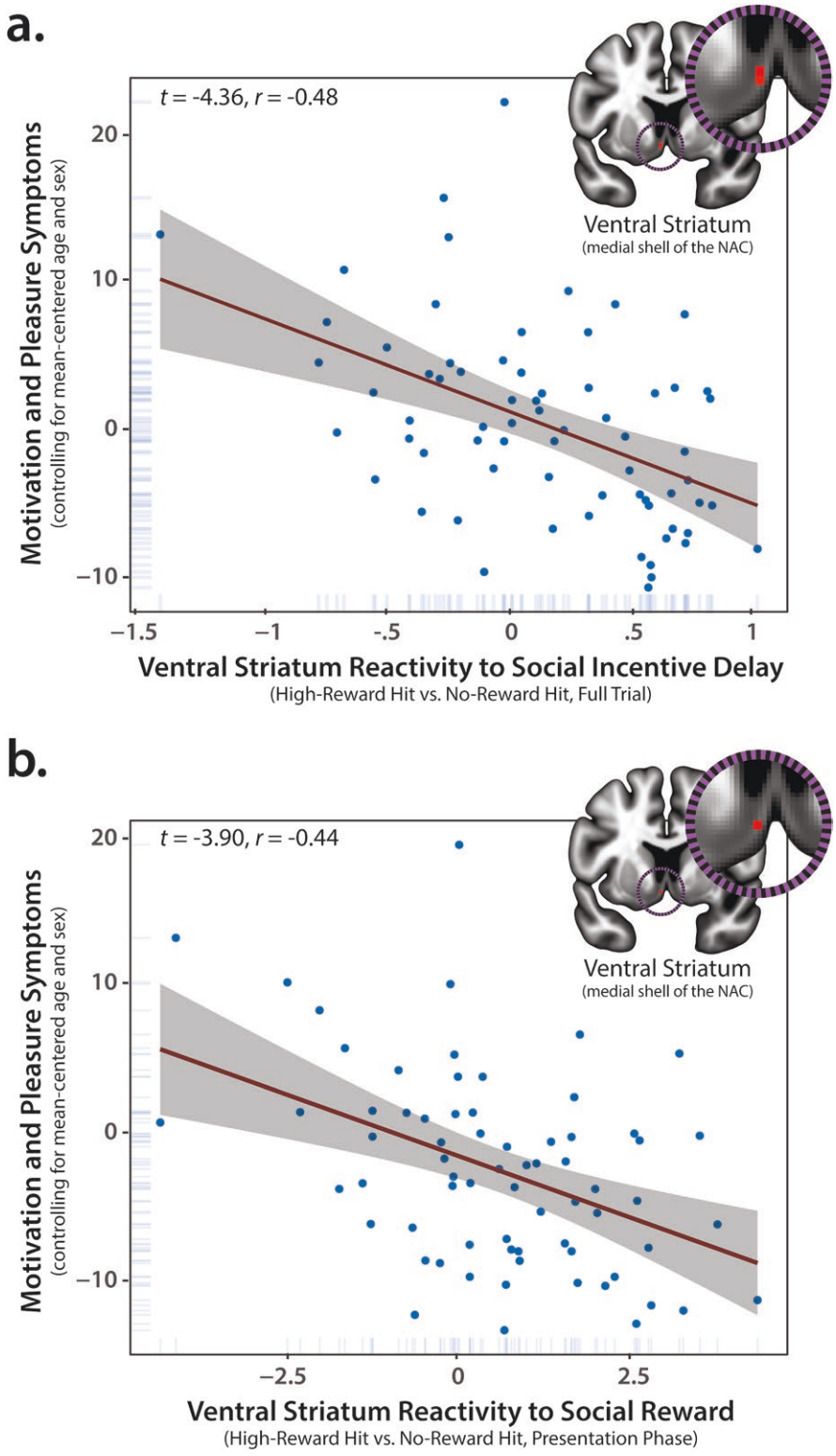

Figure 4. Blunted Ventral Striatum Reactivity to Naturalistic Social Incentives is Associated With More Severe Clinician-Rated MAP Deficits. (a) Decreased Ventral Striatum Activation During High-Reward SID Trials is Associated With More Severe MAP Symptoms. The Peak Lies in the Region of the Medial Shell of the Nucleus Accumbens ($x = -4$, $y = 6$, $z = -8$; cf. **Figure 1**). (b) Decreased Activation During the Presentation Phase of High-Reward SID Trials is Associated With More Severe MAP Symptoms in an Overlapping Region of the Ventral Striatum (red) ($x = -4$, $y = 6$, $z = -8$). Red lines depict the regression slope for the peak voxel. Gray envelopes depict 95% confidence intervals. Dots and ticks indicate individual participants. Analyses controlled for mean-centered age and biological sex ($P < .05$ FWE corrected for the volume of the anatomically defined ventral striatum). Key conclusions remained unchanged for analyses employing robust regression. Abbreviations: Corr., Corrected for the Volume of the Anatomically Defined Ventral Striatum; FWE, Familywise Error; MAP, Motivation-and-Pleasure Symptoms (CAINS); NAC, Nucleus Accumbens; SID, Social Incentive Delay Paradigm.

The present results extend prior work from our team focused on affiliative deficits in psychosis spectrum disorders. We reported that MAP deficits undermine the neuroregulatory benefits of social affiliation in the face of acute threat.[15] Taken with the current findings, these studies indicate that more severe MAP symptoms are broadly related to diminished neural responses typically associated with affiliation and social reward. Furthermore, our findings across these 2 studies suggest that in the social sphere, pleasure-related deficits in psychosis spectrum disorders can occur in the consummatory phase and are not limited to the anticipatory phase.[101,102] More broadly, these observations add to a growing body of empirical work—encompassing laboratory emotion inductions,[103] retrospective questionnaires,[22] and real-world experience sampling[104]—that challenges the popular notion that MAP deficits in psychosis are unrelated to acute ("in-the-moment") hedonic responses to normatively pleasurable stimuli.[105] Psychosis spectrum disorders are notoriously heterogeneous, and it is unlikely that deficits in consummatory pleasure are universal. Indeed, a recent large-scale meta-analysis ($N = 6913$) of emotion-induction studies demonstrated that attenuated responses to positive stimuli are most pronounced among individuals with more severe negative symptoms,[103] echoing the brain-symptom associations reported here.

Clearly, important challenges remain. First, our study was focused on a relatively large community sample that was heavily enriched for stable psychosis (**Table 1**). While this enabled us to assess a broad range of cross-cutting MAP symptoms, enhancing power and transdiagnostic relevance, it precludes direct comparison with prior neuroimaging research focused on small case-control samples (median $N = 28$, median $n_{Cases} = 20$).[23,91,106] Moving forward, it will be important to expand our naturalistic approach to encompass larger, more nationally representative samples; to explore potential case-control, diagnostic, and demographic (eg, gender) differences; and to examine paradigms that incorporate genuine, real-time social feedback.[39,107] It will also be fruitful to assess subjective responses (eg, hedonic pleasure, wanting, and positive affect) to the incentive stimuli. Second, most participants were on a stable regimen of outpatient treatment. Although this enhances clinical relevance, the potential impact of medications on our findings is unknown. Because medication types and dosages were clinically determined and the actual degree of adherence was not ascertained, we cannot determine what impact, if any, medication may have had.[108] It merits comment that 13% of our sample—or nearly 1 in 5 clinical participants—was taking typical antipsychotic medications (**Table 1**), which antagonize dopamine D2 receptors, and have been associated with depression, anhedonia, and diminished reward sensitivity.[109,110] It will be useful to determine whether ventral striatum reactivity to social incentives is blunted in unmedicated individuals and whether it is rescued by switching to atypical antipsychotics or the recently approved muscarinic agonist, xanomeline, which has shown efficacy at reducing negative symptoms.[100,110,111] Third, MAP deficits likely reflect multiple distributed neural circuits. Indeed, ventral striatal reactivity to social incentives statistically explained less than one-quarter of the variance in MAP symptoms (**Figure 4a**). A key challenge for the future will be to determine how interactions between the ventral striatum and other regions implicated in appetitive motivation and hedonic pleasure support variation in MAPS symptoms. Fourth, the absence of punishment trials precludes strong claims about valence.[112] While unlikely, similar associations might be evident for negative social feedback. Fifth, contrary to expectation, we did not detect significant associations between ventral striatum reactivity to social or monetary incentives and self-reported social functioning. In retrospect, this likely reflects the limitations of our focal measure (SLOF). Among individuals with psychotic disorders, self-reported social functioning shows weak convergence with clinician ratings ($r = 0.15$ for the SLOF) and, in contrast to clinician ratings, negligible associations with objective behavioral measures.[113,114] It will be helpful for future research to adopt a broader approach (eg, high-contact clinicians, semi-structured behavioral assessments, and experience sampling).[115]

In sum, the present study leveraged matched SID/MID fMRI paradigms and naturalistic social rewards to demonstrate that MAP symptoms are preferentially associated with blunted ventral striatum reactivity during the receipt of social reward. These observations provide fresh neurobiological insights into the social-anhedonia symptoms and social impairment that afflict many individuals living with psychotic disorders.[1–6,19,116,117] While established treatments often fail to alleviate these symptoms—making this a critical unmet need[7,95,118–120]—our results underscore the potential benefit of emerging interventions targeting positive affect, hedonic pleasure, and social affiliation.[100]

Supplementary Material

Supplementary material is available at https://academic.oup.com/schizophreniabulletin.

Acknowledgments

The authors acknowledge critical feedback and assistance from L. Friedman, the Laboratory of Emotion and Psychopathology, the Maryland Neuroimaging Center, Cornerstone Montgomery Clinics, and seven anonymous reviewers.

Author Contributions

Conceptualization: J.B., M.B., J.S., and J.M.; Methodology: J.B., J.S., R.O., C.S., and J.M.; Analysis: J.S., A.S., and J.B.; Investigation: R.O., C.S., and J.S.; Writing—Original Draft Preparation: A.S., J.B., J.S., P.D., and R.O.; Writing—Review & Editing: All authors; Funding Acquisition: J.B. and M. B.; Project Administration: J.B., M.B., and R.O.

Funding

This work was supported by the National Institutes of Health (MH110462 (Blanchard), AA030042 (Shackman), AA031261 (Shackman), MH102870 (McCarthy), MH121409 (Blanchard, Shackman), MH131264 (Shackman), DA050808 (McCarthy) and the University of Maryland.

Conflicts of Interest

None declared.

Data Availability

De-identified raw data are publicly available (https://nda.nih.gov/edit_collection.html?id=2480).

References

1. Cloutier B, Francoeur A, Samson C, Ghostine A, Lecomte T. Romantic relationships, sexuality, and psychotic disorders: a systematic review of recent findings. *Psychiatr Rehabil J.* 2021;44:22–42. https://doi.org/10.1037/prj0000409
2. Green MF, Horan WP, Lee J, McCleery A, Reddy LF, Wynn JK. Social disconnection in schizophrenia and the general community. *Schizophr Bull.* 2018;44:242–249. https://doi.org/10.1093/schbul/sbx082
3. Gooding DC, Pflum M. The transdiagnostic nature of social anhedonia: historical and current perspectives. *Curr Topics Behav Neurosci.* 2022;58:381–395. https://doi.org/10.1007/7854_2021_301
4. Koutra K, Triliva S, Roumeliotaki T, Basta M, Lionis C, Vgontzas AN. Family functioning in first-episode and chronic psychosis: the role of patient's symptom severity and psychosocial functioning. *Community Ment Health J.* 2016;52:710–723. https://doi.org/10.1007/s10597-015-9916-y
5. Velthorst E, Fett AJ, Reichenberg A, et al. The 20-year longitudinal trajectories of social functioning in individuals with psychotic disorders. *Am J Psychiatry.* 2017;174:1075–1085. https://doi.org/10.1176/appi.ajp.2016.15111419
6. Ventura J, Subotnik KL, Gitlin MJ, et al. Negative symptoms and functioning during the first year after a recent onset of schizophrenia and 8 years later. *Schizophr Res.* 2015;161:407–413. https://doi.org/10.1016/j.schres.2014.10.043
7. Cella M, Roberts S, Pillny M, et al. Psychosocial and behavioural interventions for the negative symptoms of schizophrenia: a systematic review of efficacy meta-analyses. *Br J Psychiatry*. 2023;223:321–331. https://doi.org/10.1192/bjp.2023.21
8. Devoe DJ, Braun A, Seredynski T, Addington J. Negative symptoms and functioning in youth at risk of psychosis: a systematic review and meta-analysis. *Harv Rev Psychiatry.* 2020;28:341–355.
9. Blanchard JJ, Park SG, Catalano LT, Bennett ME. Social affiliation and negative symptoms in schizophrenia: examining the role of behavioral skills and subjective responding. *Schizophr Res.* 2015;168:491–497. https://doi.org/10.1016/j.schres.2015.07.019
10. Kring AM, Gur RE, Blanchard JJ, Horan WP, Reise SP. The clinical assessment interview for negative symptoms (CAINS): final development and validation. *Am J Psychiatry.* 2013;170:165–172. https://doi.org/10.1176/appi.ajp.2012.12010109
11. McCarthy JM, Bradshaw KR, Catalano LT, et al. Negative symptoms and the formation of social affiliative bonds in schizophrenia. *Schizophr Res.* 2018;193:225–231. https://doi.org/10.1016/j.schres.2017.07.034
12. Hu H, Liu C, Zhang J, et al. A transdiagnostic network analysis of motivation and pleasure, expressivity and social functioning. *Nat Mental Health.* 2023;1:586–595. https://doi.org/10.1038/s44220-023-00102-3
13. Catalano LT, Green MF. Social motivation in schizophrenia: what's effort got to do with it? *Schizophr Bull.* 2023;49:1127–1137. https://doi.org/10.1093/schbul/sbad090
14. Moe AM, Weiss DM, Pine JG, Wastler HM, Breitborde NJK. Social motivation and behavior in first-episode psychosis: unique contributions to social quality of life and social functioning. *J Psychiatr Res.* 2021;144:441–447. https://doi.org/10.1016/j.jpsychires.2021.11.001
15. Blanchard JJ, Smith JF, Bennett ME, et al. Reward and motivation deficits undermine the benefits of social affiliation in psychosis. *Clin Psychol Sci*. 2024;12:1195–1217. https://doi.org/10.1177/21677026241227886
16. Kasanova Z, Oorschot M, Myin-Germeys I. Social anhedonia and asociality in psychosis revisited. An experience sampling study. *Psychiatry Res.* 2018;270:375–381. https://doi.org/10.1016/j.psychres.2018.09.057
17. Kalin M, Kaplan S, Gould F, Pinkham AE, Penn DL, Harvey PD. Social cognition, social competence, negative symptoms and social outcomes: inter-relationships in people with schizophrenia. *J Psychiatr Res.* 2015;68:254–260. https://doi.org/10.1016/j.jpsychires.2015.07.008
18. Taylor CT, Stein MB, Simmons AN, et al. Amplification of positivity treatment for anxiety and depression: a randomized experimental therapeutics trial targeting social reward sensitivity to enhance social connectedness. *Biol Psychiatry.* 2024;95:434–443. https://doi.org/10.1016/j.biopsych.2023.07.024
19. Abplanalp SJ, Green MF, Wynn JK, et al. Using machine learning to understand social isolation and loneliness in schizophrenia, bipolar disorder, and the community. *Schizophrenia (Heidelberg, Germany)*. 2024;10:88. https://doi.org/10.1038/s41537-024-00511-y
20. Moran EK, Culbreth AJ, Barch DM. Anhedonia in schizophrenia. *Curr Topics Behav Neurosci.* 2022;58:129–145. https://doi.org/10.1007/7854_2022_321
21. Fulford D, Campellone T, Gard DE. Social motivation in schizophrenia: how research on basic reward processes informs and limits our understanding. *Clin Psychol Rev.* 2018;63:12–24. https://doi.org/10.1016/j.cpr.2018.05.007

22. Visser KF, Chapman HC, Ruiz I, Raugh IM, Strauss GP. A meta-analysis of self-reported anticipatory and consummatory pleasure in the schizophrenia-spectrum. *J Psychiatr Res.* 2020;121:68–81. https://doi.org/10.1016/j.jpsychires.2019.11.007
23. Zeng J, Yan J, Cao H, et al. Neural substrates of reward anticipation and outcome in schizophrenia: a meta-analysis of fMRI findings in the monetary incentive delay task. *Transl Psychiatry.* 2022;12:448. https://doi.org/10.1038/s41398-022-02201-8
24. Strauss GP, Bartolomeo LA, Harvey PD. Avolition as the core negative symptom in schizophrenia: relevance to pharmacological treatment development. *npj Schizophr.* 2021;7:16. https://doi.org/10.1038/s41537-021-00145-4
25. Mow JL, Gandhi A, Fulford D. Imaging the "social brain" in schizophrenia: a systematic review of neuroimaging studies of social reward and punishment. *Neurosci Biobehav Rev.* 2020;118:704–722. https://doi.org/10.1016/j.neubiorev.2020.08.005
26. Heimer LA. New anatomical framework for neuropsychiatric disorders and drug abuse. *Am J Psychiatry.* 2003;160:1726–1739. https://doi.org/10.1176/appi.ajp.160.10.1726
27. Voorn P, Brady LS, Berendse HW, Richfield EK. Densitometrical analysis of opioid receptor ligand binding in the human striatum–I. Distribution of mu opioid receptor defines shell and core of the ventral striatum. *Neuroscience.* 1996;75:777–792. https://doi.org/10.1016/0306-4522(96)00271-0
28. Fox AS, Chang LJ, Gorgolewski KJ, Yarkoni T. Bridging psychology and genetics using large-scale spatial analysis of neuroimaging and neurogenetic data. *bioRxiv*. 2014. https://doi.org/10.1101/012310, December 9, 2014, preprint: not peer reviewed.
29. Berridge KC, Kringelbach ML. Pleasure systems in the brain. *Neuron.* 2015;86:646–664. https://doi.org/10.1016/j.neuron.2015.02.018
30. Morales I, Berridge KC. "Liking" and 'wanting' in eating and food reward: brain mechanisms and clinical implications. *Physiol Behav.* 2020;227:113152. https://doi.org/10.1016/j.physbeh.2020.113152
31. Mai JK, Majtanik M, Paxinos G. *Atlas of the Human Brain*. 4th ed. Academic Press; 2015.
32. Ding SL, Royall JJ, Sunkin SM, et al. Comprehensive cellular-resolution atlas of the adult human brain. *J Comp Neurol.* 2016;524:3127–3481. https://doi.org/10.1002/cne.24080
33. Nielson DM, Keren H, O'Callaghan G, et al. Great expectations: a critical review of and suggestions for the study of reward processing as a cause and predictor of depression. *Biol Psychiatry.* 2021;89:134–143. https://doi.org/10.1016/j.biopsych.2020.06.012
34. Lee J, Jimenez AM, Reavis EA, Horan WP, Wynn JK, Green MF. Reduced neural sensitivity to social vs nonsocial reward in schizophrenia. *Schizophr Bull.* 2019;45:620–628. https://doi.org/10.1093/schbul/sby109
35. Schwarz K, Moessnang C, Schweiger JI, et al. Transdiagnostic prediction of affective, cognitive, and social function through brain reward anticipation in schizophrenia, bipolar disorder, major depression, and autism spectrum diagnoses. *Schizophr Bull.* 2020;46:592–602. https://doi.org/10.1093/schbul/sbz075
36. Jimenez AM, Clayson PE, Hasratian AS, et al. Neuroimaging of social motivation during winning and losing: associations with social anhedonia across the psychosis spectrum. *Neuropsychologia.* 2023;188:108621. https://doi.org/10.1016/j.neuropsychologia.2023.108621
37. Clark LA, Cuthbert B, Lewis-Fernandez R, Narrow WE, Reed GM. Three approaches to understanding and classifying mental disorder: ICD-11, DSM-5, and the national institute of mental health's Research Domain Criteria (RDoC). *Psychol Sci Public Interest*. 2017;18:72–145. https://doi.org/10.1177/1529100617727266
38. Tiego J, Martin E, DeYoung CG, et al. Precision behavioral phenotyping as a strategy for uncovering the biological correlates of psychopathology. *Nat Mental Health*. 2023;1:304–315. https://doi.org/10.31219/osf.io/geh6q
39. Redcay E, Schilbach L. Using second-person neuroscience to elucidate the mechanisms of social interaction. *Nat Rev Neurosci.* 2019;20:495–505. https://doi.org/10.1038/s41583-019-0179-4
40. Blanchard JJ, Andrea A, Orth RD, Savage C, Bennett ME. Sleep disturbance and sleep-related impairment in psychotic disorders are related to both positive and negative symptoms. *Psychiatry Res.* 2020;286:112857. https://doi.org/10.1016/j.psychres.2020.112857
41. Blanchard JJ, Savage CLG, Orth RD, Jacome AM, Bennett ME. Sleep problems and social impairment in psychosis: a transdiagnostic study examining multiple social domains. *Front Psychiatry.* 2020;11:486. https://doi.org/10.3389/fpsyt.2020.00486
42. Savage CLG, Orth RD, Jacome AM, Bennett ME, Blanchard JJ. Assessing the psychometric properties of the PROMIS sleep measures in persons with psychosis. *Sleep.* 2021;44:zsab140. https://doi.org/10.1093/sleep/zsab140
43. First MB, Williams JBW, Karg RS, Spitzer RL. *Structured clinical interview for DSM-5—Research version (SCID-5 for DSM-5, research version; SCID-5-RV)*. Arlington, VA: American Psychiatric Association. 2015;
44. Horan WP, Kring AM, Gur RE, Reise SP, Blanchard JJ. Development and psychometric validation of the Clinical Assessment Interview for Negative Symptoms (CAINS). *Schizophr Res.* 2011;132:140–145. https://doi.org/10.1016/j.schres.2011.06.030
45. Engel M, Lincoln TM. Concordance of self- and observer-rated motivation and pleasure in patients with negative symptoms and healthy controls. *Psychiatry Res.* 2017;247:1–5. https://doi.org/10.1016/j.psychres.2016.11.013
46. Xie DJ, Shi HS, Lui SSY, et al. Cross cultural validation and extension of the Clinical Assessment Interview for Negative Symptoms (CAINS) in the Chinese Context: evidence from a spectrum perspective. *Schizophr Bull.* 2018;44:S547–S555. https://doi.org/10.1093/schbul/sby013
47. Blanchard JJ, Bradshaw KR, Garcia CP, et al. Examining the reliability and validity of the clinical assessment interview for negative symptoms within the management of schizophrenia in clinical practice (MOSAIC) multisite national study. *Schizophr Res.* 2017;185:137–143. https://doi.org/10.1016/j.schres.2017.01.011
48. Kopelowicz A, Ventura J, Liberman RP, Mintz J. Consistency of brief psychiatric rating scale factor structure across a broad spectrum of schizophrenia patients. *Psychopathology.* 2008;41:77–84. https://doi.org/10.1159/000111551
49. Ventura J, Lukoff D, Nuechterlein KH, Liberman RP, Green MF, Shaner A. Brief Psychiatric Rating Scale (BPRS), expanded version (4.0): scales, anchor points, and administration. Manual. *Int J Methods Psychiatric Res*. 1993;3:227–243.
50. Harvey PD, Raykov T, Twamley EW, Vella L, Heaton RK, Patterson TL. Validating the measurement of real-world functional outcomes: phase I results of the VALERO study. *Am J Psychiatry.* 2011;168:1195–1201.

51. Schneider LC, Struening EL. SLOF: a behavioral rating scale for assessing the mentally ill. *Social Work Res Abstracts*. 1983;19:9–21.
52. Spreckelmeyer KN, Krach S, Kohls G, et al. Anticipation of monetary and social reward differently activates mesolimbic brain structures in men and women. *Soc Cogn Affect Neurosci*. 2009;4:158–165. https://doi.org/10.1093/scan/nsn051
53. Knutson B, Westdorp A, Kaiser E, Hommer D. FMRI visualization of brain activity during a monetary incentive delay task. *Neuroimage*. 2000;12:20–27.
54. Kohls G, Perino MT, Taylor JM, et al. The nucleus accumbens is involved in both the pursuit of social reward and the avoidance of social punishment. *Neuropsychologia*. 2013;51:2062–2069. https://doi.org/10.1016/j.neuropsychologia.2013.07.020
55. Krause F, Benjamins C, Eck J, Lührs M, van Hoof R, Goebel R. Active head motion reduction in magnetic resonance imaging using tactile feedback. *Hum Brain Mapp*. 2019;40:4026–4037.
56. Cox RW. AFNI: software for analysis and visualization of functional magnetic resonance neuroimages. *Comput Biomed Res Int J*. 1996;29:162–173.
57. Kim HC, Kaplan CM, Islam S, et al. Acute nicotine abstinence amplifies subjective withdrawal symptoms and threat-evoked fear and anxiety, but not extended amygdala reactivity. *PLoS One*. 2023;18:e0288544. https://doi.org/10.1371/journal.pone.0288544
58. Hur J, Kuhn M, Grogans SE, et al. Anxiety-related frontocortical activity is associated with dampened stressor reactivity in the real world. *Psychol Sci*. 2022;33:906–924. https://doi.org/10.1101/2021.03.17.435791
59. Tustison NJ, Avants BB, Cook PA, et al. N4ITK: improved N3 bias correction. Article. *IEEE Trans Med Imag*. 2010;29:1310–1320. https://doi.org/10.1109/tmi.2010.2046908
60. Avants BB, Tustison NJ, Song G, Cook PA, Klein A, Gee JC. A reproducible evaluation of ANTs similarity metric performance in brain image registration. Article. *Neuroimage*. 2011;54:2033–2044. https://doi.org/10.1016/j.neuroimage.2010.09.025
61. Eskildsen SF, Coupé P, Fonov V, et al.; Alzheimer's Disease Neuroimaging Initiative. BEaST: brain extraction based on nonlocal segmentation technique. *Neuroimage*. 2012;59:2362–2373.
62. BIAC. IXI Dataset. Imperial College London. Accessed April 19, 2022. https://brain-development.org/ixi-dataset/
63. Grabner G, Janke AL, Budge MM, Smith D, Pruessner J, Collins DL. Symmetric atlasing and model based segmentation: an application to the hippocampus in older adults. *Med Image Comput Computer-Assisted Interven*. 2006;9:58–66. https://doi.org/10.1007/11866763_8
64. Lorio S, Fresard S, Adaszewski S, et al. New tissue priors for improved automated classification of subcortical brain structures on MRI. *Neuroimage*. 2016;130:157–166. https://doi.org/10.1016/j.neuroimage.2016.01.062
65. Jenkinson M, Beckmann CF, Behrens TE, Woolrich MW, Smith SM. FSL. *Neuroimage*. 2012;62:782–790. https://doi.org/10.1016/j.neuroimage.2011.09.015
66. McCormick M, Liu X, Jomier J, Marion C, Ibanez L. ITK enabling reproducible research and open science. *Front Neuroinf*. 2014;8:13. https://doi.org/10.3389/fninf.2014.00013
67. Dohmatob E, Varoquaux G, Thirion B. Inter-subject registration of functional images: do we need anatomical images? *Front Neurosci*. 2018;12:64. https://doi.org/10.3389/fnins.2018.00064
68. Grabner G, Poser BA, Fujimoto K, et al. A study-specific fMRI normalization approach that operates directly on high resolution functional EPI data at 7 Tesla. *Neuroimage*. 2014;100:710–714. https://doi.org/10.1016/j.neuroimage.2014.06.045
69. Huang CM, Lee SH, Hsiao IT, et al. Study-specific EPI template improves group analysis in functional MRI of young and older adults. *J Neurosci Methods*. 2010;189:257–266. https://doi.org/10.1016/j.jneumeth.2010.03.021
70. Wellcome Centre for Human Neuroimaging. SPM. University College London. Accessed April 18, 2022. https://fil.ion.ucl.ac.uk/spm/
71. Pruim RHR, Mennes M, van Rooij D, Llera A, Buitelaar JK, Beckmann CF. ICA-AROMA: a robust ICA-based strategy for removing motion artifacts from fMRI data. *Neuroimage*. 2015;112:267–277.
72. Mumford JA, Poline JB, Poldrack RA. Orthogonalization of regressors in fMRI models. *PLoS One*. 2015;10:e0126255. https://doi.org/10.1371/journal.pone.0126255
73. Tukey JW. *Exploratory Data Analysis*. Addison Wesley; 1977.
74. Wager TD, Keller MC, Lacey SC, Jonides J. Increased sensitivity in neuroimaging analyses using robust regression. *Neuroimage*. 2005;26:99–113. S1053-8119(05)00036-4 [pii] https://doi.org/10.1016/j.neuroimage.2005.01.011
75. R Core Team. *R: A Language and Environment for Statistical Computing*. R Foundation for Statistical Computing; 2022.
76. RStudio Team. *RStudio: Integrated Development for R*. RStudio PBC; 2022.
77. Wickham H. *ggplot2: Elegant graphics for data analysis*. 2nd ed. Springer-Verlag; 2016.
78. Rorden C. MRIcron. NITRC. Updated September 2, 2019. Accessed April 18, 2022. https://www.nitrc.org/projects/mricron
79. Desikan RS, Ségonne F, Fischl B, et al. An automated labeling system for subdividing the human cerebral cortex on MRI scans into gyral based regions of interest. *Neuroimage*. 2006;31:968–980.
80. Frazier JA, Chiu S, Breeze JL, et al. Structural brain magnetic resonance imaging of limbic and thalamic volumes in pediatric bipolar disorder. *Am J Psychiatry*. 2005;162:1256–1265.
81. Makris N, Goldstein JM, Kennedy D, et al. Decreased volume of left and total anterior insular lobule in schizophrenia. *Schizophr Res*. 2006;83:155–171.
82. Mackey S, Petrides M. Architecture and morphology of the human ventromedial prefrontal cortex. *Eur J Neurosci*. 2014;40:2777–2796. https://doi.org/10.1111/ejn.12654
83. ten Donkelaar HJ, Tzourio-Mazoyer N, Mai JK. Toward a common terminology for the gyri and sulci of the human cerebral cortex. Review. *Front Neuroanat*. 2018;12:93. https://doi.org/10.3389/fnana.2018.00093
84. Morel A, Loup F, Magnin M, Jeanmonod D. Neurochemical organization of the human basal ganglia: anatomofunctional territories defined by the distributions of calcium-binding proteins and SMI-32. *J Comp Neurol*. 2002;443:86–103. https://doi.org/10.1002/cne.10096
85. Eklund A, Nichols TE, Knutsson H. Cluster failure: why fMRI inferences for spatial extent have inflated false-positive rates. *Proc Natl Acad Sci USA*. 2016;113:7900–7905. https://doi.org/10.1073/pnas.1602413113
86. Tziortzi AC, Searle GE, Tzimopoulou S, et al. Imaging dopamine receptors in humans with [11C]-(+)-PHNO: dissection

of D3 signal and anatomy. *Neuroimage.* 2011;54:264–277. https://doi.org/10.1016/j.neuroimage.2010.06.044

87. Shackman AJ, Fox AS, Oler JA, et al. Heightened extended amygdala metabolism following threat characterizes the early phenotypic risk to develop anxiety-related psychopathology. *Mol Psychiatry.* 2017;22:724–732.
88. Schuyler BS, Kral TR, Jacquart J, et al. Temporal dynamics of emotional responding: amygdala recovery predicts emotional traits. *Soc Cogn Affect Neurosci*. 2014;9:176–181. https://doi.org/10.1093/scan/nss131
89. Oldham S, Murawski C, Fornito A, Youssef G, Yücel M, Lorenzetti V. The anticipation and outcome phases of reward and loss processing: a neuroimaging meta-analysis of the monetary incentive delay task. *Hum Brain Mapp.* 2018;39:3398–3418. https://doi.org/10.1002/hbm.24184
90. Chen Y, Chaudhary S, Li CR. Shared and distinct neural activity during anticipation and outcome of win and loss: a meta-analysis of the monetary incentive delay task. *Neuroimage.* 2022;264:119764. https://doi.org/10.1016/j.neuroimage.2022.119764
91. Wang X, Zhang Y, Huang J, et al. Revisiting reward impairments in schizophrenia spectrum disorders: a systematic review and meta-analysis for neuroimaging findings. *Psychol Med.* 2023;53:7189–7202. https://doi.org/10.1017/s0033291723000703
92. Cicero DC, Ruggero CJ, Balling CE, et al. State of the science: the hierarchical taxonomy of psychopathology (HiTOP). *Behav Ther*. 2024;55:1114–1129. https://doi.org/10.1016/j.beth.2024.05.001, preprint: not peer reviewed.
93. Eaton NR, Bringmann LF, Elmer T, et al. A review of approaches and models in psychopathology conceptualization research. *Nat Rev Psychol.* 2023;2:622–636. https://doi.org/10.1038/s44159-023-00218-4
94. Heimer L. Basal forebrain in the context of schizophrenia. *Brain Res Brain Res Rev.* 2000;31:205–235. https://doi.org/10.1016/s0165-0173(99)00039-9
95. Galderisi S, Mucci A, Buchanan RW, Arango C. Negative symptoms of schizophrenia: new developments and unanswered research questions. *Lancet Psychiatry*. 2018;5:664–677. https://doi.org/10.1016/s2215-0366(18)30050-6
96. Buchel C, Miedl S, Sprenger C. Hedonic processing in humans is mediated by an opioidergic mechanism in a mesocorticolimbic system. *Elife*. 2018;7:e39648. https://doi.org/10.7554/eLife.39648
97. Best MW, Bowie CR. Social exclusion in psychotic disorders: an interactional processing model. *Schizophr Res.* 2022;244:91–100. https://doi.org/10.1016/j.schres.2022.05.016
98. Penn DL, Kohlmaier JR, Corrigan PW. Interpersonal factors contributing to the stigma of schizophrenia: social skills, perceived attractiveness, and symptoms. *Schizophr Res.* 2000;45:37–45. https://doi.org/10.1016/s0920-9964(99)00213-3
99. Riehle M, Mehl S, Lincoln TM. The specific social costs of expressive negative symptoms in schizophrenia: reduced smiling predicts interactional outcome. *Acta Psychiatr Scand.* 2018;138:133–144. https://doi.org/10.1111/acps.12892
100. Craske MG, Dunn BD, Meuret AE, Rizvi SJ, Taylor CT. Positive affect and reward processing in the treatment of depression, anxiety and trauma. *Nat Rev Psychol*. 2024;3:665–685. https://doi.org/10.1038/s44159-024-00355-4
101. Engel M, Fritzsche A, Lincoln TM. Anticipation and experience of emotions in patients with schizophrenia and negative symptoms. An experimental study in a social context. *Schizophr Res.* 2016;170:191–197. https://doi.org/10.1016/j.schres.2015.11.028
102. Gard DE, Kring AM, Gard MG, Horan WP, Green MF. Anhedonia in schizophrenia: distinctions between anticipatory and consummatory pleasure. *Schizophr Res.* 2007;93:253–260. https://doi.org/10.1016/j.schres.2007.03.008
103. Riehle M, Straková A, Lincoln TM. Emotional experience of people with schizophrenia and people at risk for psychosis: a meta-analysis. *JAMA Psychiatry.* 2024;81:57–66. https://doi.org/10.1001/jamapsychiatry.2023.3589
104. Abel DB, Rand KL, Salyers MP, Myers EJ, Mickens JL, Minor KS. Do people with schizophrenia enjoy social activities as much as everyone else? A meta-analysis of consummatory social pleasure. *Schizophr Bull.* 2023;49:809–822. https://doi.org/10.1093/schbul/sbac199
105. Kring AM, Moran EK. Emotional response deficits in schizophrenia: insights from affective science. *Schizophr Bull.* 2008;34:819–834. https://doi.org/10.1093/schbul/sbn071
106. Radua J, Schmidt A, Borgwardt S, et al. Ventral striatal activation during reward processing in psychosis: a neurofunctional meta-analysis. *JAMA Psychiatry*. 2015;72:1243–1251. https://doi.org/10.1001/jamapsychiatry.2015.2196
107. Schilbach L, Redcay E. Synchrony across brains. *Annu Rev Psychol.* in press. https://doi.org/10.1146/annurev-psych-080123-101149
108. Blanchard JJ, Neale JM. Medication effects: conceptual and methodological issues in schizophrenia research. *Clin Psychol Rev.* 1992;12:345–361. https://doi.org/10.1016/0272-7358(92)90141-T
109. Berg M, Riehle M, Rief W, Lincoln TM. Does partial blockade of dopamine D2 receptors with Amisulpride cause anhedonia? An experimental study in healthy volunteers. *J Psychiatr Res.* 2023;158:409–416. https://doi.org/10.1016/j.jpsychires.2023.01.014
110. Juckel G. Inhibition of the reward system by antipsychotic treatment. *Dialogues Clin Neurosci.* 2016;18:109–114. https://doi.org/10.31887/DCNS.2016.18.1/gjuckel
111. Horan WP, Targum SD, Claxton A, et al. Efficacy of KarXT on negative symptoms in acute schizophrenia: a post hoc analysis of pooled data from 3 trials. *Schizophr Res.* 2024;274:57–65. https://doi.org/10.1016/j.schres.2024.08.001
112. Dugré JR, Dumais A, Bitar N, Potvin S. Loss anticipation and outcome during the monetary incentive delay task: a neuroimaging systematic review and meta-analysis. *PeerJ.* 2018;6:e4749. https://doi.org/10.7717/peerj.4749
113. Sabbag S, Twamley EW, Vella L, Heaton RK, Patterson TL, Harvey PD. Predictors of the accuracy of self assessment of everyday functioning in people with schizophrenia. *Schizophr Res.* 2012;137:190–195. https://doi.org/10.1016/j.schres.2012.02.002
114. Sabbag S, Twamley EM, Vella L, Heaton RK, Patterson TL, Harvey PD. Assessing everyday functioning in schizophrenia: not all informants seem equally informative. *Schizophr Res.* 2011;131:250–255. https://doi.org/10.1016/j.schres.2011.05.003
115. Abel DB, Minor KS. Social functioning in schizophrenia: comparing laboratory-based assessment with real-world measures. *J Psychiatr Res.* 2021;138:500–506. https://doi.org/10.1016/j.jpsychires.2021.04.039
116. Trøstheim M, Eikemo M, Meir R, et al. Assessment of anhedonia in adults with and without mental illness: a systematic review and meta-analysis. *JAMA Netw Open.* 2020;3:e2013233. https://doi.org/10.1001/jamanetworkopen.2020.13233

117. Husain M, Roiser JP. Neuroscience of apathy and anhedonia: a transdiagnostic approach. *Nat Rev Neurosci.* 2018;19:470–484. https://doi.org/10.1038/s41583-018-0029-9

118. Pizzagalli DA. Toward a better understanding of the mechanisms and pathophysiology of anhedonia: are we ready for translation? *Am J Psychiatry.* 2022;179:458–469. https://doi.org/10.1176/appi.ajp.20220423

119. Craske MG, Meuret AE, Echiverri-Cohen A, Rosenfield D, Ritz T. Positive affect treatment targets reward sensitivity: a randomized controlled trial. *J Consult Clin Psychol.* 2023;91:350–366. https://doi.org/10.1037/ccp0000805

120. Sandman CF, Craske MG. Psychological treatments for anhedonia. *Curr Topics Behav Neurosci.* 2022;58:491–513. https://doi.org/10.1007/7854_2021_291

Supplementary Figure and Results

Alexander J. Shackman[1,2,3]
Jason F. Smith*[1]
Ryan D. Orth[1]
Christina L. G. Savage[1]
Paige R. Didier[1]
Julie M. McCarthy[4,5]
Melanie E. Bennett[6]
Jack J. Blanchard*[1]

Department of [1]Psychology, [2]Neuroscience and Cognitive Science Program, and [3]Maryland Neuroimaging Center, University of Maryland, College Park, MD 20742, USA. [4]Division of Psychotic Disorders, McLean Hospital, Belmont, MA 02478 USA. [5]Department of Psychiatry, Harvard Medical School, Boston, MA 02115 USA. [6]Department of Psychiatry, University of Maryland School of Medicine, Baltimore, MD 21201, USA.

* contributed equally

Please address manuscript correspondence to

Dr. Jack J. Blanchard (jblancha@umd.edu)

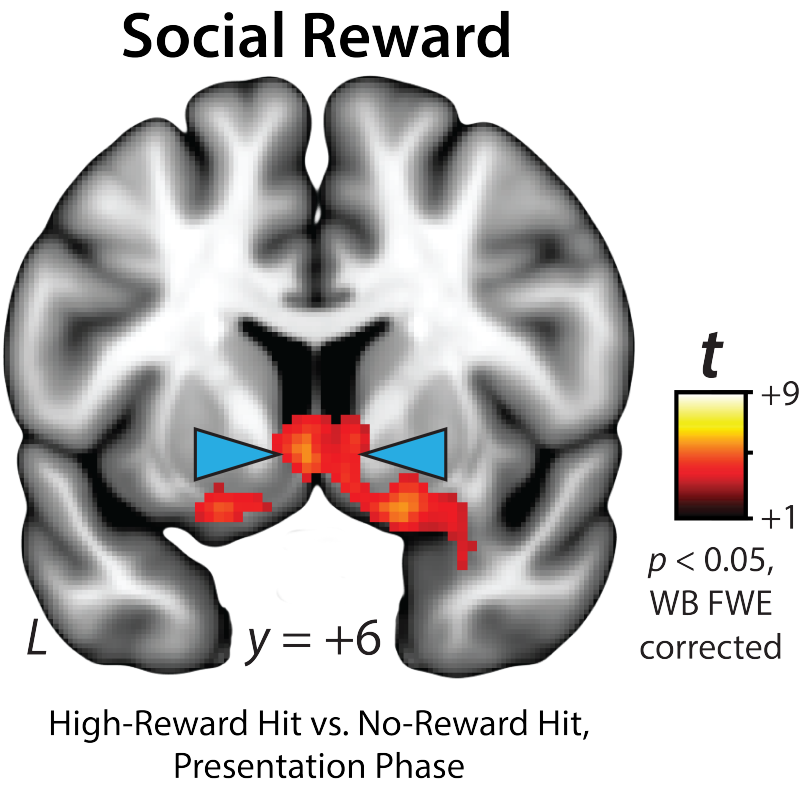

Supplementary Figure S1. ***The presentation of social reward robustly engages the ventral striatum.*** Regions showing significantly greater activation during High- compared to No-Reward hit trials during the presentation phase of the SID paradigm (p<0.05, whole-brain FWE corrected). Significant activation was not evident in the ventral striatum during the anticipation phase, even when using a more liberal small-volume threshold (p<0.05, ventral striatum FWE corrected). Blue arrows indicate the ventral striatum. **Abbreviations**—FWE, familywise error; L, left hemisphere; SID, social incentive delay; WB, whole-brain.

Supplementary Table S1. Descriptive statistics for clusters and local extrema showing greater activation in the SID paradigm for High-Reward compared to No-Reward hit trials (p<0.05, whole-brain FWE corrected).

		mm³	***t***	***x***	***y***	***z***
Cluster 1		60480				
	R Lateral Occipital Cortex, inferior division		17.14	46	-68	2
	R Occipital Pole		13.21	16	-92	6
	R Occipital Fusiform Gyrus		12.81	30	-76	-12
	R Temporal Occipital Fusiform Cortex		10.2	46	-50	-16
	R Inferior Temporal Gyrus, temporooccipital part		8.68	48	-58	-14
	R Lateral Occipital Cortex, superior division		8.04	28	-84	22
	R Temporal Fusiform Cortex, posterior division		6.55	38	-38	-22
Cluster 2		31168				
	L Lateral Occipital Cortex, inferior division		13.18	-44	-70	4
	L Temporal Occipital Fusiform Cortex		7.68	-40	-56	-14
	L Temporal Fusiform Cortex, posterior division		6.22	-40	-36	-24
	L Occipital Pole		5.29	-24	-94	-8
	L Occipital Fusiform Gyrus		5.21	-32	-80	-14
	L Lateral Occipital Cortex, superior division		4.75	-42	-88	12
Cluster 3		12368				
	L Paracingulate Gyrus		6.33	-2	46	4
	L Cingulate Gyrus, anterior division		5.7	-6	36	20
	L Frontal Pole		3.56	-4	62	6
	R Cingulate Gyrus, anterior division		6.83	6	30	14
	R Paracingulate Gyrus		6.3	4	46	10
	R Frontal Medial Cortex		3.64	0	50	-8
Cluster 4		8792				
	L Frontal Orbital Cortex		4.78	-26	14	-20
	L Left Thalamus		4.52	-6	-2	4
	L Insular Cortex		4.15	-32	16	-10
	R Ventral Striatum		7.56	8	14	-6
	R Ventral Striatum		7.05	10	14	-8
	R Insular Cortex		5.02	36	20	-8
	R Right Caudate		3.49	6	12	6
Cluster 5		3136				

	L Brain-Stem		4.45	-6	-36	-6
	R Brain-Stem		5.38	6	-36	-8
	R Right Thalamus		5.33	10	-30	-2
Cluster 6		1888				
	R Superior Parietal Lobule		5.39	26	-52	52
	R Lateral Occipital Cortex, superior division		3.96	22	-62	46
Cluster 7		1280				
	R Heschl's Gyrus (includes H1 and H2)		4.43	46	-20	8
	R Planum Temporale		4.25	62	-16	4
Cluster 8		792				
	L Lateral Occipital Cortex, superior division		4.38	-30	-72	22

Supplementary Table S2. Descriptive statistics for clusters and local extrema showing greater activation in the SID paradigm for No-Reward compared to High-Reward hit trials ($p<0.05$, whole-brain FWE corrected).

		mm³	***t***	***x***	***y***	***z***
No Clusters						

Supplementary Table S3. Descriptive statistics for clusters and local extrema showing greater activation in the MID paradigm for High-Reward compared to No-Reward hit trials (p<0.05, whole-brain FWE corrected).

		mm³	***t***	***x***	***y***	***z***
Cluster 1		99568				
	L Lateral Occipital Cortex, inferior division		9.36	-48	-78	-10
	L Occipital Fusiform Gyrus		6.19	-36	-70	-18
	L Occipital Pole		5.77	-38	-90	8
	L Lateral Occipital Cortex, superior division		5.72	-40	-88	10
	L Intracalcarine Cortex		4.92	-12	-82	8
	L Lingual Gyrus		4.69	-4	-72	4
	L Middle Temporal Gyrus, temporooccipital part		3.87	-56	-58	8
	L Inferior Temporal Gyrus, temporooccipital part		3.81	-48	-62	-20
	R Lateral Occipital Cortex, inferior division		9.32	44	-80	-8
	R Occipital Pole		6.85	12	-90	2
	R Inferior Temporal Gyrus, temporooccipital part		6.35	56	-60	-10
	R Middle Temporal Gyrus, temporooccipital part		6.24	58	-54	-8
	R Occipital Fusiform Gyrus		5.76	30	-70	-18
	R Lateral Occipital Cortex, superior division		5.22	40	-80	12
	R Intracalcarine Cortex		5.11	6	-74	6
	R Lingual Gyrus		4.53	12	-62	2
	R Brain-Stem		3.91	12	-44	-40
Cluster 2		61112				
	L Frontal Orbital Cortex		5.98	-28	22	-10
	L Insular Cortex		5.49	-38	14	-6
	L Frontal Operculum Cortex		5.11	-34	20	10
	L Brain-Stem		4.62	-4	-34	-26
	L Thalamus		3.55	-6	-26	12
	R Frontal Orbital Cortex		7.67	32	30	-2
	R Middle Frontal Gyrus		7.39	44	6	36
	R Thalamus		6.57	2	-12	12
	R Precentral Gyrus		6.48	42	8	26
	R Brain-Stem		5.81	4	-32	-18
	R Inferior Frontal Gyrus, pars opercularis		5.1	50	8	16
	R Caudate		4.57	14	-6	18
	R Insular Cortex		4.38	38	6	-4

	R Putamen		4.2	30	-12	-10
	R Amygdala		4.07	26	0	-12
	R Superior Frontal Gyrus		3.91	24	8	66
	R Pallidum		3.76	24	-8	-6
	R Ventral Striatum		8.78	12	14	-10
	L Ventral Striatum		7.81	-10	14	-10
	L Ventral Striatum		8.32	-6	16	-4
	R Ventral Striatum		9.23	8	14	-2
Cluster 3		35000				
	L Cingulate Gyrus, anterior division		7.14	-2	34	20
	L Paracingulate Gyrus		6.96	-2	38	28
	L Cingulate Gyrus, posterior division		4.84	-8	-22	42
	L Juxtapositional Lobule Cortex (formerly Supplementary Motor Cortex)		4.31	-2	6	58
	R Paracingulate Gyrus		7.04	2	36	26
	R Cingulate Gyrus, anterior division		6.96	0	46	4
	R Cingulate Gyrus, posterior division		5.12	0	-32	26
Cluster 4		23992				
	R Superior Parietal Lobule		7.56	32	-48	48
	R Supramarginal Gyrus, posterior division		7.16	48	-38	54
	R Lateral Occipital Cortex, superior division		6.36	26	-68	38
	R Supramarginal Gyrus, anterior division		5.08	56	-26	44
	R Precuneus Cortex		4.16	16	-66	38
Cluster 5		8592				
	L Precentral Gyrus		6.89	-54	0	48
	L Superior Frontal Gyrus		4.62	-22	0	54
	L Inferior Frontal Gyrus, pars opercularis		4.34	-56	10	16
Cluster 6		6096				
	L Lateral Occipital Cortex, superior division		5.5	-28	-66	30
	L Superior Parietal Lobule		4.57	-28	-52	48
	L Precuneus Cortex		4.33	-6	-78	54
Cluster 7		1176				
	L Supramarginal Gyrus, posterior division		4.97	-56	-42	22

Supplementary Table S4. Descriptive statistics for clusters and local extrema showing greater activation in the MID paradigm for No-Reward compared to High-Reward hit trials (p<0.05, whole-brain FWE corrected).

		mm³	***t***	***x***	***y***	***z***
Cluster 1		5784				
	R Planum Temporale		6.02	56	-26	10
	R Heschl's Gyrus (includes H1 and H2)		5.87	38	-22	12
	R Insular Cortex		5.05	38	-16	16
	R Central Opercular Cortex		3.94	56	-8	8
	R Postcentral Gyrus		3.89	66	-6	28
Cluster 2		1840				
	L Central Opercular Cortex		5.62	-36	-20	20
	L Heschl's Gyrus (includes H1 and H2)		4.97	-36	-28	14
Cluster 3		1048				
	R Occipital Pole		4.51	22	-96	4
Cluster 4		904				
	R Precentral Gyrus		4.78	4	-28	66

Supplementary Table S5 Descriptive statistics for clusters and local extrema showing greater activation in the SID paradigm for the anticipation of High-Reward compared to No-Reward incentives (p<0.05, whole-brain FWE corrected).

		mm³	***t***	***x***	***y***	***z***
Cluster 1	R Occipital Fusiform Gyrus	4976	9.09	30	-76	-10
	R Temporal Occipital Fusiform Cortex		6.38	30	-54	-10
	R Lingual Gyrus		5.55	26	-60	-4
Cluster 2	L Occipital Fusiform Gyrus	4824	8.96	-30	-72	-12
	L Lingual Gyrus		6.13	-24	-58	-8
	L Temporal Occipital Fusiform Cortex		5.21	-28	-54	-10
Cluster 3	L Left Thalamus	2072	3.76	-6	-22	2
	R Right Thalamus		4.97	4	-14	2
	R Brain-Stem		4.07	6	-30	-6
Cluster 4	L Juxtapositional Lobule Cortex (formerly Supplementary Motor Cortex)	1352	4.39	-6	2	48
	L Cingulate Gyrus, anterior division		3.49	-6	12	36
	R Juxtapositional Lobule Cortex (formerly Supplementary Motor Cortex)		3.87	2	-4	58
Cluster 5	R Juxtapositional Lobule Cortex (formerly Supplementary Motor Cortex)	888	4.90	10	6	44
	R Cingulate Gyrus, anterior division		3.70	8	-8	42

Supplementary Table S6 Descriptive statistics for clusters and local extrema showing greater activation in the SID paradigm for the anticipation of No-Reward compared to High-Reward incentives (p<0.05, whole-brain FWE corrected).

		mm³	***t***	***x***	***y***	***z***
Cluster 1	R Lateral Occipital Cortex, superior division	5400	4.89	42	-72	44
	R Angular Gyrus		4.30	56	-58	20
Cluster 2	L Lateral Occipital Cortex, superior division	3840	4.59	-46	-70	26
Cluster 3	R Lateral Occipital Cortex, inferior division	3000	5.61	50	-64	-14
	R Inferior Temporal Gyrus, temporooccipital part		4.29	48	-50	-18
	R Temporal Occipital Fusiform Cortex		3.55	44	-42	-24
Cluster 4	R Middle Temporal Gyrus, anterior division	1768	4.87	64	-6	-20
	R Middle Temporal Gyrus, posterior division		4.46	66	-14	-26
Cluster 5	L Amygdala	1248	5.19	-26	-10	-16
	L Amygdala		3.82	-28	0	-26
	L Amygdala		3.56	-24	0	-20
	L Amygdala		5.19	-26	-10	-16
Cluster 6	L Superior Frontal Gyrus	1112	3.97	-16	34	54
Cluster 7	R Lingual Gyrus	992	4.41	18	-52	2
	R Cingulate Gyrus, posterior division		4.32	16	-48	4
	R Precuneus Cortex		3.76	6	-60	10
Cluster 8	R Frontal Pole	744	4.50	2	64	0

Supplementary Table S7. Descriptive statistics for clusters and local extrema showing greater activation in the SID paradigm for the presentation of High-Reward compared to No-Reward incentives (p<0.05, whole-brain FWE corrected).

		mm³	***t***	***x***	***y***	***z***
Cluster 1		82944				
	R Lateral Occipital Cortex, inferior division		17.92	48	-70	0
	R Occipital Pole		12.8	16	-92	4
	R Temporal Occipital Fusiform Cortex		11.61	44	-50	-20
	R Inferior Temporal Gyrus, temporooccipital part		10.49	48	-60	-14
	R Occipital Fusiform Gyrus		10.47	22	-86	-10
	R Lateral Occipital Cortex, superior division		8.9	30	-84	26
	R Planum Temporale		6.27	62	-12	4
	R Supramarginal Gyrus, posterior division		5.01	66	-42	14
	R Heschl's Gyrus (includes H1 and H2)		4.58	50	-18	6
	R Superior Temporal Gyrus, anterior division		3.67	64	0	-8
Cluster 2		38008				
	L Lateral Occipital Cortex, inferior division		13.02	-48	-72	4
	L Temporal Occipital Fusiform Cortex		8.03	-42	-54	-22
	L Occipital Pole		7.86	-24	-96	0
	L Occipital Fusiform Gyrus		5.01	-34	-80	-18
	L Lateral Occipital Cortex, superior division		4.89	-40	-88	12
	L Supramarginal Gyrus, posterior division		4.19	-56	-50	14
	L Inferior Temporal Gyrus, temporooccipital part		3.94	-60	-46	-16
Cluster 3		19456				
	R Amygdala		5.83	28	2	-14
	R Amygdala		5.25	24	-6	-12
	R Amygdala		5.09	16	-6	-14
	R Amygdala/ R Parahippocampal Gyrus, anterior division		4.71	26	0	-30
	R Amygdala		3.55	22	-4	-26
	L Amygdala		5.76	-14	-6	-18
	L Amygdala		4.78	-28	-8	-14
	L Amygdala		4.67	-22	0	-26
	L Frontal Orbital Cortex		6.23	-26	14	-20

	L Insular Cortex		4.84	-30	14	-10
	L Parahippocampal Gyrus, anterior division		4.25	-16	-6	-26
	L Hippocampus		4.14	-32	-8	-22
	L Thalamus		3.85	-16	-34	-2
	L Putamen		3.46	-20	14	2
	R Thalamus		5.97	12	-32	0
	R Hippocampus		5.16	20	-30	-6
	R Temporal Pole		3.54	30	6	-24
	R Putamen		3.39	32	-12	-2
	R Ventral Striatum		5.49	10	10	-12
	R Ventral Striatum		5.99	6	12	-6
	R Ventral Striatum		7.56	8	14	-6
	R Ventral Striatum		5.89	8	16	-6
Cluster 4		15744				
	L Paracingulate Gyrus		5.34	-2	34	-10
	L Cingulate Gyrus, anterior division		5.23	-6	32	-4
	L Caudate		4.16	-10	10	16
	L Frontal Pole		4.05	-2	58	-6
	R Cingulate Gyrus, anterior division		6.51	0	46	4
	R Frontal Pole		5.37	0	62	6
	R Subcallosal Cortex		5.06	2	28	-20
	R Frontal Medial Cortex		4.49	2	52	-8
	R Paracingulate Gyrus		4.05	8	46	18
Cluster 5		3224				
	L Frontal Pole		5.3	-12	46	50
	L Superior Frontal Gyrus		4.81	-18	38	46
Cluster 6		1600				
	L Cingulate Gyrus, posterior division		3.85	-4	-46	32
	R Cingulate Gyrus, posterior division		4.09	0	-30	32
Cluster 7		1368				
	R Superior Parietal Lobule		5.41	30	-50	54

Supplementary Table S8. Descriptive statistics for clusters and local extrema showing greater activation in the SID paradigm for the presentation of No-Reward compared to High-Reward incentives (p<0.05, whole-brain FWE corrected).

		mm³	***t***	***x***	***y***	***z***
Cluster 1		3568				
	R Frontal Pole		5.1	30	40	28
Cluster 2		2888				
	L Juxtapositional Lobule Cortex (formerly Supplementary Motor Cortex)		4.99	-2	-10	54
	R Juxtapositional Lobule Cortex (formerly Supplementary Motor Cortex)		4.72	8	4	54
Cluster 3		2016				
	L Precentral Gyrus		4.61	-26	-14	70
Cluster 4		1584				
	R Postcentral Gyrus		4.48	54	-16	40
	R Supramarginal Gyrus, anterior division		4.4	62	-30	38
Cluster 5		1304				
	R Superior Frontal Gyrus		5.01	26	2	60
Cluster 6		1040				
	L Postcentral Gyrus		4.59	-40	-28	62
Cluster 7		904				
	R Cingulate Gyrus, posterior division		5.18	12	-24	40
Cluster 8		704				
	L Postcentral Gyrus		4.74	-58	-16	50

Supplementary Table S9. Descriptive statistics for clusters and local extrema showing greater activation in the MID paradigm for the anticipation of High-Reward compared to No-Reward incentives (p<0.05, whole-brain FWE corrected).

		mm³	***t***	***x***	***y***	***z***
Cluster 1	L Precentral Gyrus	55544	6.04	-50	-10	44
	L Juxtapositional Lobule Cortex (formerly Supplementary Motor Cortex)		5.87	-2	-2	56
	L Postcentral Gyrus		5.78	-36	-28	66
	L Cingulate Gyrus, anterior division		5.63	-6	8	40
	L Superior Parietal Lobule		4.51	-30	-42	62
	L Superior Frontal Gyrus		4.04	-20	4	72
	R Juxtapositional Lobule Cortex (formerly Supplementary Motor Cortex)		6.57	10	0	54
	R Precentral Gyrus		5.61	46	-8	54
	R Cingulate Gyrus, anterior division		4.76	6	10	28
	R Superior Frontal Gyrus		4.74	20	6	56
	R Cingulate Gyrus, posterior division		4.68	12	-16	40
	R Precuneus Cortex		4.52	8	-48	60
	R Postcentral Gyrus		3.85	12	-40	58
Cluster 2	L Brain-Stem	26384	6.81	-4	-30	-14
	L Ventral Striatum		4.39	-6	6	-2
	L Thalamus		6.00	-2	-16	6
	L Caudate		4.83	-14	20	-2
	L Putamen		4.42	-20	10	-2
	L Pallidum		3.69	-14	-2	-2
	R Thalamus		7.16	4	-16	6
	R Brain-Stem		6.85	4	-28	-2
	Midline Left Thalamus		5.52	0	-6	2
	R Caudate		5.31	10	8	-2
	R Pallidum		4.23	18	4	0
	R Putamen		3.99	18	12	-12
Cluster 3	L Occipital Fusiform Gyrus	18416	9.57	-26	-82	-10
	L Occipital Pole		6.26	-12	-100	-2
	L Temporal Occipital Fusiform Cortex		5.51	-30	-52	-14
	L Lateral Occipital Cortex, inferior division		4.55	-30	-86	2
	L Lateral Occipital Cortex, superior division		3.85	-30	-88	22
	L Lingual Gyrus		3.45	-22	-46	-6

Cluster 4	R Occipital Fusiform Gyrus	18072	10.17	32	-72	-12
	R Temporal Occipital Fusiform Cortex		6.47	34	-54	-16
	R Occipital Pole		6.22	14	-90	-4
	R Lateral Occipital Cortex, inferior division		4.64	36	-76	8
Cluster 5	L Heschls Gyrus (includes H1 and H2)	4664	7.54	-46	-22	6
	L Planum Temporale		6.80	-40	-32	10
	L Parietal Operculum Cortex		4.91	-32	-28	20
Cluster 6	R Heschls Gyrus (includes H1 and H2)	2496	6.38	52	-16	4
	R Planum Temporale		5.04	40	-28	14
Cluster 7	R Insular Cortex	2008	5.14	32	26	-2
	R Frontal Operculum Cortex		4.49	34	24	6
Cluster 8	L Insular Cortex	1712	4.89	-30	26	2
	L Frontal Operculum Cortex		4.27	-32	22	12
Cluster 9	L Brain-Stem	1600	5.92	-2	-36	-40
	R Brain-Stem		3.96	2	-32	-30
Cluster 10	R Intracalcarine Cortex	928	4.74	8	-72	16

Supplementary Table S10. Descriptive statistics for clusters and local extrema showing greater activation in the MID paradigm for the anticipation of No-Reward compared to High-Reward incentives (p<0.05, whole-brain FWE corrected).

		mm³	***t***	***x***	***y***	***z***
Cluster 1	L Paracingulate Gyrus	4648	5.87	-2	50	-6
	L Frontal Pole		4.36	-2	60	22
	L Frontal Medial Cortex		4.34	-2	46	-14
	L Cingulate Gyrus, anterior division		3.87	-4	40	-4
	R Frontal Pole		4.62	2	60	-6
	R Paracingulate Gyrus		3.78	4	52	12
Cluster 2	L Superior Frontal Gyrus	3672	5.96	-12	28	60
	L Frontal Pole		4.55	-10	42	52
	L Middle Frontal Gyrus		4.26	-42	22	40
Cluster 3	L Lateral Occipital Cortex, superior division	3384	4.62	-46	-62	28
Cluster 4	L Precuneus Cortex	2952	5.29	-10	-54	34
	L Cingulate Gyrus, posterior division		4.04	-14	-48	0
	R Precuneus Cortex		3.57	4	-54	16
Cluster 5	R Lateral Occipital Cortex, superior division	2824	4.65	48	-70	42
	R Angular Gyrus		3.28	54	-58	40
Cluster 6	R Superior Frontal Gyrus	2432	5.28	20	28	58
	R Middle Frontal Gyrus		4.31	34	26	50
	R Frontal Pole		3.67	22	38	48
Cluster 8	R Middle Temporal Gyrus, posterior division	800	4.19	62	-10	-14

Supplementary Table S11. Descriptive statistics for clusters and local extrema showing greater activation in the MID paradigm for the presentation of High-Reward compared to No-Reward incentives (p<0.05, whole-brain FWE corrected).

		mm³	***t***	***x***	***y***	***z***
Cluster 1	R Amygdala	164232	4.81	26	-2	-12
	R Amygdala		4.80	24	-14	-10
	R Amygdala		3.99	30	-4	-22
	L Lateral Occipital Cortex, inferior division		9.20	-48	-76	-10
	L Lingual Gyrus		8.27	-6	-76	-14
	L Subcallosal Cortex		7.70	-2	14	-2
	L Lateral Occipital Cortex, superior division		5.90	-40	-86	12
	L Inferior Temporal Gyrus, posterior division		5.70	-54	-42	-18
	L Middle Temporal Gyrus, temporooccipital part		5.17	-60	-62	0
	L Thalamus		5.15	-10	-2	10
	L Inferior Temporal Gyrus, temporooccipital part		4.98	-48	-54	-20
	L Occipital Fusiform Gyrus		4.96	-42	-66	-16
	L Intracalcarine Cortex		4.53	-10	-88	0
	R Lateral Occipital Cortex, inferior division		8.54	44	-80	-8
	R Supramarginal Gyrus, posterior division		8.32	48	-40	54
	R Inferior Temporal Gyrus, temporooccipital part		7.82	48	-60	-8
	R Superior Parietal Lobule		6.80	38	-46	52
	R Caudate		6.53	6	10	-2
	R Thalamus		6.53	2	-10	12
	R Lateral Occipital Cortex, superior division		6.37	30	-64	30
	R Intracalcarine Cortex		6.21	12	-88	2
	R Parahippocampal Gyrus, posterior division		5.69	20	-26	-12
	R Lingual Gyrus		5.51	12	-68	-10
	R Cingulate Gyrus, posterior division		5.19	10	-42	2
	R Middle Temporal Gyrus, posterior division		4.86	64	-28	-18
	R Amygdala		4.81	26	-2	-12
	R Occipital Pole		4.51	2	-96	8
	R Middle Temporal Gyrus, temporooccipital part		4.28	66	-40	-8
	R Brain-Stem		3.32	10	-44	-48
Cluster 2	L Paracingulate Gyrus	29104	6.98	-10	38	18

	R Cingulate Gyrus, anterior division		8.64	0	46	4
	R Frontal Orbital Cortex		6.72	40	20	-8
	R Paracingulate Gyrus		6.47	2	36	28
	R Insular Cortex		5.10	40	12	-8
	R Frontal Pole		3.45	24	42	-10
Cluster 3	L Supramarginal Gyrus, anterior division	11528	5.82	-48	-38	42
	L Supramarginal Gyrus, posterior division		5.32	-50	-44	54
	L Lateral Occipital Cortex, superior division		5.27	-26	-72	34
	L Superior Parietal Lobule		5.12	-36	-54	52
Cluster 4	R Precentral Gyrus	7760	7.52	42	8	28
	R Inferior Frontal Gyrus, pars opercularis		6.60	54	12	30
	R Middle Frontal Gyrus		5.56	54	10	40
Cluster 5	L Cingulate Gyrus, anterior division	7016	6.60	-2	0	34
	R Cingulate Gyrus, anterior division		6.48	0	-10	38
	R Cingulate Gyrus, posterior division		6.36	0	-32	26
Cluster 6	L Precentral Gyrus	5768	6.05	-48	8	28
	L Inferior Frontal Gyrus, pars opercularis		4.12	-50	10	20
	L Central Opercular Cortex		4.08	-36	-2	18
Cluster 7	L Insular Cortex	4584	5.63	-34	14	-8
	L Frontal Orbital Cortex		4.78	-36	18	-16
	L Temporal Pole		4.19	-52	4	-6
	L Planum Polare		3.98	-56	-2	0
Cluster 8	L Insular Cortex	1288	5.17	-36	-6	-6
	L Putamen		4.48	-30	-18	6
Cluster 9	L Parietal Operculum Cortex	1128	4.55	-52	-40	24
	L Supramarginal Gyrus, posterior division		3.99	-56	-42	32

Supplementary Table S12. Descriptive statistics for clusters and local extrema showing greater activation in the MID paradigm for the presentation of No-Reward compared to High-Reward incentives (p<0.05, whole-brain FWE corrected).

		mm³	***t***	***x***	***y***	***z***
Cluster 1	L Precentral Gyrus	7888	4.79	-4	-16	64
	L Postcentral Gyrus		4.26	-6	-38	62
	R Juxtapositional Lobule Cortex (formerly Supplementary Motor Cortex)		5.89	4	-12	68
	R Precentral Gyrus		5.70	4	-28	66
	R Postcentral Gyrus		3.46	34	-28	66
Cluster 2	R Occipital Fusiform Gyrus	5024	9.01	28	-78	-10
	R Occipital Pole		5.23	22	-96	2
Cluster 3	R Planum Temporale	4616	6.85	40	-28	16
	R Insular Cortex		5.02	36	-18	16
	R Heschls Gyrus (includes H1 and H2)		4.21	50	-10	2
	R Central Opercular Cortex		3.91	46	-12	12
Cluster 4	L Heschls Gyrus (includes H1 and H2)	4240	7.07	-36	-26	12
	L Insular Cortex		6.47	-34	-24	18
	L Planum Temporale		6.15	-40	-34	10
	L Parietal Operculum Cortex		5.87	-32	-30	20
Cluster 5	L Occipital Fusiform Gyrus	3600	7.92	-26	-76	-10
	L Occipital Pole		5.09	-16	-94	-6
Cluster 6	R Thalamus	856	5.60	16	-24	4